Octet baryon electromagnetic form factors in nuclear medium

G. Ramalho[1], K. Tsushima[2], and A. W. Thomas[2,3]

[1] CFTP, Instituto Superior Técnico, Universidade Técnica de Lisboa, Av. Rovisco Pais, 1049-001 Lisboa, Portugal
[2]CSSM and [3]CoEPP, School of Chemistry and Physics, University of Adelaide, Adelaide SA 5005, Australia

Abstract. We study the octet baryon electromagnetic form factors in nuclear matter using the covariant spectator quark model extended to the nuclear matter regime. The parameters of the model in vacuum are fixed by the study of the octet baryon electromagnetic form factors. In nuclear matter the changes in hadron properties are calculated by including the relevant hadron masses and the modification of the pion-baryon coupling constants calculated in the quark-meson coupling model. In nuclear matter the magnetic form factors of the octet baryons are enhanced in the low Q^2 region, while the electric form factors show a more rapid variation with Q^2. The results are compared with the modification of the bound proton electromagnetic form factors observed at Jefferson Lab. In addition, the corresponding changes for the bound neutron are predicted.

PACS numbers: 13.40.Gp, 21.65.-f, 14.20.Jn, 12.39.Ki

1. Introduction

Whether or not hadrons change their properties in a nuclear medium, has been one of the long-standing problems in nuclear physics [1, 2]. QCD is established as the theory of strong interactions and quarks and gluons are the degrees of freedom in the QCD Lagrangian. It seems natural that in the strong mean fields which pervade nuclear matter the motion of the quarks and gluons inside hadrons should be modified. Such changes are what is meant by the nuclear modification of hadron properties and studying such effect is clearly central to the understanding of dense matter within QCD.

Recently, strong evidence concerning the modification of nucleon properties in a nuclear medium has been reported from the proton electromagnetic form factors measured in polarized $(\vec{e}, e'\vec{p})$ scattering on ^{16}O [3] and ^{4}He [4, 5, 6, 7] at MAMI and Jefferson Lab. These experiments measured the double ratio of proton-recoil polarization transfer coefficients in the quasi-elastic scattering off nuclei, and the results were normalized with respective to the double ratio of hydrogen. The results from ^{4}He strongly suggest the modification of the bound proton electromagnetic form factors. Furthermore, the study of neutron properties in the nuclear medium in [8], predicts an enhancement of the same double ratio for the neutron, contrary to the suppression observed for the proton. The corresponding experiment, to measure the polarization transfer, is planned in the future [9]. Theoretically, there are several studies concerning the electromagnetic form factors of the nucleon in

the nuclear medium [8, 10, 11, 12, 13]. They are based either on quark degrees of freedom [8, 10, 11, 12], or meson and nucleon degrees of freedom [13]. However, it is very difficult to separate and identify the observed effects in terms of these degrees of freedom. In particular, to distinguish a possible change in the nucleon properties in a nuclear medium from those of the conventional many-body effects, such as final state interactions and meson exchange current, are very difficult, and seems only possible in a model dependent way, where experimental measurement involves all such effects including the one-body current modification [2, 14, 15]. Thus, the interpretation of the modification observed is still under discussion and has not been settled yet. In these circumstances it is helpful to examine the modification of the electromagnetic form factors of the nucleon and other baryons in the nuclear medium within alternative approaches.

In this article we study the medium modification of the the octet baryon electromagnetic form factors in nuclear matter focusing on the valence quark structure of a baryon. Thus, we do not include final state interactions nor meson exchange current, where the latter may possibly be important for the magnetic form factors of baryons in a nucleus and nuclear matter [13, 14, 16, 17, 18, 19]. For this purpose, we use the covariant spectator quark model [20, 21, 22, 23, 24], which has its basis in the covariant spectator theory [25]. The model has been successfully applied to study the electromagnetic properties of the octet [26, 27] and decuplet [28, 29, 30, 31, 32] baryons. The model was also very successful in the studies of $\gamma^* N \to \Delta(1232)$ [33, 34, 35, 36], $\gamma^* N \to N(1440)$ [37], and $\gamma^* N \to N(1535)$ [38] reactions. For the meson cloud effects, we include the pion cloud effects, which are expected to be dominant, in a phenomenological manner based on the method applied in [24, 26, 27].

In [27] the model was extended to the lattice regime to utilize the lattice QCD simulation data, where the electromagnetic form factors of the octet baryons were able to be calculated at lattice hadron masses corresponding to large pion mass values used in the lattice QCD simulations. Similarly, it is also possible to extend the model to the in-medium regime, once we are able to calculate the in-medium modified masses of the baryons and mesons appearing in the model. This is the working hypothesis used to extend the model, and to calculate the in-medium modifications of the octet baryon electromagnetic form factors. For the in-medium masses of the baryons and mesons, we use the quark-meson coupling (QMC) model [39, 40], which has been successfully applied to study the properties of nuclei [41, 42], hypernuclei [43, 44, 45, 46], and hadron properties in a nuclear medium [47], based on the relativistic valence quark structure of hadrons in a nuclear medium.

Another point to note concerning this study is that the parametrization of the pion cloud contributions in vacuum has been improved over what was used in the past [27] based on lattice QCD simulation and chiral perturbation theory. In particular, care is taken for the neutron charge form factor and the charge radius, where the pion cloud contributions are very important. This is also true for the electric charge neutral particles.

This paper is organized as follows. We start by defining the electromagnetic form factors in medium in section 2. In section 3 we explain the covariant spectator quark model, and describe the electromagnetic currents for octet baryons in the model. The extension of the model to the in-medium regime is discussed in section 5. Results are presented in section 6, and discussions and summary are given in section 7.

2. Electromagnetic form factors in vacuum and in the nuclear matter

A spin 1/2 baryon B, a member of the baryon octet, has a Dirac structure and therefore its electromagnetic structure can be expressed in terms of two independent form factors, namely, the electric G_{EB} and magnetic G_{MB} form factors in vacuum (mass M_B) and those in the nuclear medium (mass M_B^*) G_{EB}^* and G_{MB}^*, respectively, and they are defined below.

2.1. In vacuum

Let us consider an octet baryon B, with mass M_B in vacuum. When the initial (momentum P_-) and the final (momentum P_+) states are on-shell, the electromagnetic current (coupling of the baryon with a photon) can be represented as

$$J_B^\mu = F_{1B}(Q^2)\gamma^\mu + F_{2B}(Q^2)\frac{i\sigma^{\mu\nu}q_\nu}{2M_B}, \tag{2.1}$$

where $q = P_+ - P_-$, and F_{1B} and F_{2B} are respectively the Dirac and Pauli form factors which are the functions of $Q^2 = -q^2$.

Suppressed in equation (2.1) are the initial (u_B) and final state ($\bar{u}_B$) Dirac spinors, functions of $P_\pm$ and the spin projections. For simplicity we represent the current in units $e = \sqrt{4\pi\alpha}$, with $\alpha \simeq 1/137$, the electromagnetic fine structure constant.

At $Q^2 = 0$ they are normalized as

$$F_{1B}(0) = e_B, \qquad F_{2B}(0) = \kappa_B, \tag{2.2}$$

where e_B is the baryon charge in units of e and κ_B is the baryon anomalous magnetic moment in natural units $\frac{e}{2M_B}$.

An alternative representation of the electromagnetic form factors of the baryon B is the Sachs parametrization in terms of the electric charge G_E and magnetic dipole G_M form factors. For the electric charge form factor the following relation holds with F_{1B} and F_{2B},

$$G_{EB}(Q^2) = F_{1B}(Q^2) - \frac{Q^2}{4M_B^2}F_{2B}(Q^2). \tag{2.3}$$

As for the magnetic dipole form factor G_{MB} the natural definition is $G_{MB} = F_{1B} + F_{2B}$. At $Q^2 = 0$, $G_{MB}(Q^2)$ defines the magnetic moment of the baryon B in natural units ($\frac{e}{2M_B}$), $\mu_B = G_{MB}(0)\frac{e}{2M_B}$. To compare magnetic moments μ_B of particles with different masses it is usual to express μ_B in terms $\hat{\mu}_N = \frac{e}{2M_N}$, the nuclear magneton. In this case $\mu_B = G_{MB}(0)\frac{M_N}{M_B}\hat{\mu}_N$. Therefore, although the study of the baryon magnetic form factor can be done naturally using $G_{MB} = F_{1B} + F_{2B}$, as performed in a previous work [27], that μ_B was defined in the natural units, it is more convenient to define G_{MB} in units of the nuclear magneton. Throughout this article we will use then

$$G_{MB}(Q^2) = \left[F_{1B}(Q^2) + F_{2B}(Q^2)\right]\frac{M_N}{M_B}. \tag{2.4}$$

2.2. In medium

We consider now the octet baryon B in the nuclear medium with the effective mass M_B^*. Assuming that the baryon is quasi-free in the nuclear medium, the electromagnetic current for the baryon B can be expressed as

$$J_B^\mu = F_{1B}^*(Q^2)\gamma^\mu + F_{2B}^*(Q^2)\frac{i\sigma^{\mu\nu}q_\nu}{2M_B^*}, \tag{2.5}$$

where F^*_{1B} and F^*_{2B} are respectively the Dirac and Pauli form factors in the nuclear medium. Again the in-medium spinors $\bar{u}^*_B(P_+)$ and $u^*_B(P_-)$ are suppressed. At $Q^2 = 0$, one has also

$$F^*_{1B}(0) = e^*_B, \qquad F^*_{2B}(0) = \kappa^*_B, \tag{2.6}$$

where e^*_B is the electric charge in nuclear medium (the same as in the vacuum: $e_B = e^*_B$) and κ^*_B is the anomalous magnetic moment in units of $\frac{e}{2M^*_B}$.

As in the vacuum [see equations (2.3)-(2.4)], we define the electric charge and magnetic dipole form factors as

$$G^*_{EB}(Q^2) = F^*_{1B}(Q^2) - \frac{Q^2}{4(M^*_B)^2} F^*_{2B}(Q^2), \tag{2.7}$$

$$G^*_{MB}(Q^2) = \left[F^*_{1B}(Q^2) + F^*_{2B}(Q^2)\right] \frac{M_N}{M^*_B}. \tag{2.8}$$

Note that the nucleon mass in vacuum (M_N) is included in the definition of G^*_{MB}. As mentioned already we use this definition to make comparison easier with respect to the vacuum results.

Because the effective nucleon mass is expected to be smaller than the mass in vacuum, $M^*_N < M_N$, $G^*_{MN}(Q^2)$ is expected to increase and the magnetic moment is enhanced in magnitude ($|\mu^*_N| > |\mu_N|$).

3. Spectator quark model

We describe now the octet baryon electromagnetic form factors in vacuum for a baryon B with mass M_B following [27]. In next section we describe the extension of the model to the nuclear medium.

The electromagnetic interaction with a baryon B may be decomposed into the photon interaction with valence quarks, and with sea quarks (polarized quark-antiquark pairs or meson cloud). As the pion is the lightest meson the pion cloud is expected to give the most important contribution. Then, one can describe the electromagnetic interaction for a member B of the octet baryons using a current,

$$J^\mu_B = Z_B \left[J^\mu_{0B} + J^\mu_\pi + J^\mu_{\gamma B}\right], \tag{3.1}$$

where J^μ_{0B} stands for the electromagnetic interaction with the quark core without the pion cloud, and the remaining terms are the interaction with the intermediate pion-baryon (πB) states, as depicted in figure 1. In particular, J^μ_π represents the direct interaction with the pion [diagram (a)], and $J^\mu_{\gamma B}$ the interaction with the baryon while one pion is in the air [diagram (b)]. The factor Z_B is a renormalization constant, which is common to each isomultiplet: nucleon (N), Σ, Λ, and Ξ. Z_B is related with the derivative of the baryon self-energy [26].

We restrict the meson cloud dressing to the pion cloud, since the lightest meson is dominant as known from chiral perturbation theory. This is consistent with the studies of the octet baryon systems [48, 49, 50, 51, 52, 53, 54, 55, 56, 57, 58]. We note however, that kaon (K) cloud contributions may became more pronounced for systems with more strangeness, particularly when the pion cloud contributions are small.

In the previous work [27] we presented a model for the valence quark and meson cloud contributions that were calibrated by lattice QCD and physical nucleon electromagnetic form factor data, as well as the octet magnetic moment data (Λ,

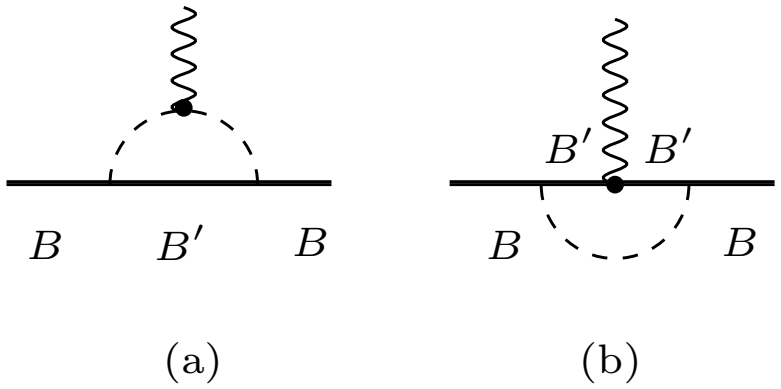

Figure 1. Electromagnetic interaction with the baryon B within the one-pion loop level through the intermediate baryon states B'. A diagram including a contact vertex $\gamma\pi BB'$, as described in [26], is not represented explicitly, since the isospin structure is the same as diagram (a). See [26] for details.

$\Sigma^{+,-}$ and $\Xi^{0,-}$). The model provided a good global description of the octet baryon electromagnetic form factor data (physical and lattice regimes) except for the neutron electric form factor in the low Q^2 region. As a consequence the model underestimated significantly the neutron electric charge square radius [-0.029 fm^2 to be compared with the experimental result -0.116 fm^2]. This was interpreted as an insufficient impact of the nucleon data in the low Q^2 region, particularly those for the neutron. Another limitation of the model was no explicit inclusion of the pion mass (m_π) in the parametrization of the pion cloud dressing. Although the long-range falloff of the pion cloud effects in the position space with the distance r going like $\exp(-2m_\pi r)$, it can be simulated by multipole functions with appropriated cutoffs. In order to study the chiral behavior, it is vital to include the pion mass dependence explicitly.

Therefore, we improve the model by adding two new features to the model of [27]:

- We constrain the model parameters using also the experimental values of the proton and neutron electric and magnetic square radii, as well as Σ^- electric square radius.
- We redefine the pion cloud parametrization in order to reproduce the leading order chiral behavior for the form factors which depend on the pion mass.

With these two additional constraints we can improve the form factors in the low Q^2 region consistently with the chiral behavior, in particular for the neutron electric form factor. We also provide a direct connection of the model with the chiral limit.

Next, we describe how the valence quark and the pion cloud contributions are integrated in the model. The explicit parametrization for the pion cloud and the connection with chiral perturbation theory are presented later.

3.1. Bare form factors

In the covariant spectator quark model a baryon B is described as a system with an off-mass-shell quark, free to interact with photons, and two on-mass-shell quarks. Integrating over the two on-mass-shell quark momenta, we represent the quark pair as an on-mass-shell diquark with an effective mass m_D, and the baryon as a quark-diquark system [20, 21]. This quark-diquark system is then described by a transition vertex

between the three-quark bound state and the quark-diquark state, that simulates the effect of confinement [20, 31].

The simplest representation for a quark-diquark system with spin 1/2 and positive parity is the S-wave configuration. As in [20, 26, 27], we represent the wavefunction Ψ_B for an octet baryon B with momentum P and the internal diquark momentum k. In the S-wave approximation the wavefunction is a combination of symmetric ($|M_S\rangle$) and anti-symmetric ($|M_A\rangle$) states in the quark pair (12), and an S-wave radial (scalar) wavefunction $\psi_B(P,k)$. The explicit expressions can be found in [27].

3.1.1. Electromagnetic current. Taking into account that the wavefunction Ψ_B is written in terms of the wavefunctions of a quark pair (12) and a single quark (3), one can write the electromagnetic current associated with the baryon B in impulse approximation [20, 31] as:

$$J^{\mu}_{0B} = 3\sum_{\Gamma}\int_{k}\overline{\Psi}_B(P_+,k)j^{\mu}_q\Psi_B(P_-,k), \tag{3.2}$$

where j^{μ}_q is the quark current operator, P_+ (P_-) is the final (initial) baryon momentum and k the momentum of the on-shell diquark. $\Gamma=\{s,\lambda\}$ labels the scalar diquark and the vectorial diquark polarization $\lambda=0,\pm$. The factor 3 in equation (3.2) takes into account the contributions for the current from the pairs (13) and (23), where each pair has an identical contribution with that of the pair (12). The polarization indices are suppressed for simplicity. The integral symbol stands for

$$\int_k \equiv \int \frac{d^3\mathbf{k}}{2E_D(2\pi)^3}, \tag{3.3}$$

where $E_D=\sqrt{m_D^2+\mathbf{k}^2}$.

Generally, the baryon electromagnetic current (3.2) can be expressed as

$$J^{\mu}_{0B} = F_{10B}(Q^2)\,\gamma^{\mu} + F_{20B}(Q^2)\,\frac{i\sigma^{\mu\nu}q_{\nu}}{2M_B}, \tag{3.4}$$

where F_{10B} and F_{20B} are respectively the valence quark contributions for the $F_{1B}(Q^2)$ and $F_{2B}(Q^2)$ form factors, defined by equation (2.1). To simplify our notations we introduce

$$\tilde{e}_{0B}\equiv F_{10B}(Q^2), \qquad \tilde{\kappa}_{0B}\equiv F_{20B}(Q^2), \tag{3.5}$$

where the tilde is included to remember that these are functions of Q^2. To represent these quantities for $Q^2=0$, respectively the charge ($\tilde{e}_{0B}$) and the anomalous magnetic moment ($\tilde{\kappa}_{0B}$) we suppress the tildes as e_{0B} and κ_{0B}.

3.1.2. Quark electromagnetic current. The quark current operator j^{μ}_q has a generic structure,

$$j^{\mu}_q = j_1\left(\gamma^{\mu}-\frac{\not{q}q^{\mu}}{q^2}\right)+j_2\frac{i\sigma^{\mu\nu}q_{\nu}}{2M_N}, \tag{3.6}$$

where M_N is the nucleon mass in vacuum and j_i ($i=1,2$) are $SU(3)$ flavor operators acting on the third quark of the $|M_A\rangle$ or $|M_S\rangle$ state. In the first term $\not{q}q^{\mu}/q^2$ is included for completeness, but does not contribute for elastic reactions.

The quark current j_i ($i=1,2$) in equation (3.6), can be decomposed as the sum of operators acting on the quark 3 in $SU(3)$ flavor space [31],

$$j_i = \tfrac{1}{6}f_{i+}\lambda_0+\tfrac{1}{2}f_{i-}\lambda_3+\tfrac{1}{6}f_{i0}\lambda_s, \tag{3.7}$$

Table 1. Mixed symmetric (j_i^S) and antisymmetric (j_i^A) coefficients for the octet baryons appearing in equations (3.8) and (3.9).

B	j_i^S	j_i^A
p	$\frac{1}{6}(f_{i+}-f_{i-})$	$\frac{1}{6}(f_{i+}+3f_{i-})$
n	$\frac{1}{6}(f_{i+}+f_{i-})$	$\frac{1}{6}(f_{i+}-3f_{i-})$
Λ	$\frac{1}{6}f_{i+}$	$\frac{1}{18}(f_{i+}-4f_{i0})$
Σ^+	$\frac{1}{18}(f_{i+}+3f_{i-}-4f_{i0})$	$\frac{1}{6}(f_{i+}+3f_{i-})$
Σ^0	$\frac{1}{36}(2f_{i+}-8f_{i0})$	$\frac{1}{6}f_{i+}$
Σ^-	$\frac{1}{18}(f_{i+}-3f_{i-}-4f_{i0})$	$\frac{1}{6}(f_{i+}-3f_{i-})$
Ξ^0	$\frac{1}{18}(2f_{i+}+6f_{i-}-2f_{i0})$	$-\frac{1}{3}f_{i0}$
Ξ^-	$\frac{1}{18}(2f_{i+}-6f_{i-}-2f_{i0})$	$-\frac{1}{3}f_{i0}$

where $\lambda_0 = \mathrm{diag}(1,1,0)$, $\lambda_3 = \mathrm{diag}(1,-1,0)$ and $\lambda_s = \mathrm{diag}(0,0,-2)$ are the flavor space operators. These operators act on the quark wavefunction in flavor space, $q = (\ u\, d\, s\ )^T$.

The functions $f_{i\pm}(Q^2)$ $(i=1,2)$ are normalized by $f_{1\,n}(0)=1$ $(n=0,\pm)$, $f_{2\pm}(0)=\kappa_\pm$, and $f_{20}(0)=\kappa_s$. The isoscalar (κ_+) and isovector (κ_-) anomalous magnetic moments are defined in terms of the u and d quark anomalous magnetic moments, $\kappa_+ = 2\kappa_u - \kappa_d$ and $\kappa_- = \frac{2}{3}\kappa_u + \frac{1}{3}\kappa_d$.

3.1.3. Dirac and Pauli bare form factors. To take into account the effect of the states with mixed symmetry in the baryon B wavefunction ($|M_A\rangle$ and $|M_S\rangle$) we sum over the quark flavors, using the coefficients [26, 27, 31],

$$j_i^A = \langle M_A|j_i|M_A\rangle, \tag{3.8}$$

$$j_i^S = \langle M_S|j_i|M_S\rangle, \tag{3.9}$$

for $i=1,2$. The expressions for j_i^A and j_i^S $(i=1,2)$ are presented in table 1 –see [27] for more details.

Using the coefficients defined by equations (3.8) and (3.9) we can write the spectator model form factors for the octet baryons characterized by a nucleon with mass M_N and the baryon B with mass M_B as [27]

$$\tilde{e}_{0B} = B(Q^2)\left(\frac{3}{2}j_1^A + \frac{1}{2}\frac{3-\tau}{1+\tau}j_1^S - 2\frac{\tau}{1+\tau}\frac{M_B}{M_N}j_2^S\right), \tag{3.10}$$

$$\tilde{\kappa}_{0B} = B(Q^2)\left[\left(\frac{3}{2}j_2^A - \frac{1}{2}\frac{1-3\tau}{1+\tau}j_2^S\right)\frac{M_B}{M_N} - 2\frac{1}{1+\tau}j_1^S\right], \tag{3.11}$$

with $\tau = \frac{Q^2}{4M_B^2}$, and

$$B(Q^2) = \int_k \psi_B(P_+,k)\psi_B(P_-,k), \tag{3.12}$$

the overlap integral between the initial and final scalar wavefunctions.

The normalization of the wavefunction [20, 27] leads to $B(0)=1$. Note that by construction the bare charge e_{0B} and the dressed charge e_B are the same, $e_{0B} \equiv e_B$.

We conclude then that the bare form factors $\tilde{e}_{0B}$ and $\tilde{\kappa}_{0B}$ are determined by the $f_{i\,n}(Q^2)$ ($i = 1, 2$, $n = 0, \pm$) and $\psi_B(P, k)$. The details of those parametrization are shown next.

We can also calculate the quark core contributions for the electric and magnetic form factors using the following expressions:

$$G_{E0B}(Q^2) = \tilde{e}_B - \tau\,\tilde{\kappa}_B, \tag{3.13}$$

$$G_{M0B}(Q^2) = [\tilde{e}_B + \tilde{\kappa}_B]\,\frac{M_N}{M_B}. \tag{3.14}$$

In equation (3.14) the factor $\frac{M_N}{M_B}$ is included to be consistent with the definition of G_{MB}.

Equations (3.10) and (3.11) can be used either in vacuum or in medium. In medium we may just replace the vacuum masses M_N and M_B respectively by the effective masses M_N^* and M_B^*. The same procedure should also be carried out in the coefficients j_i^A and j_i^S ($i = 1, 2$), namely, the vector meson masses in vacuum should be replaced by those in medium. As for equations (3.13) and (3.14) the same rules are applied except that the factor $\frac{M_N}{M_B}$ in vacuum should be replaced by $\frac{M_N}{M_B^*}$ in medium (with the nucleon vacuum mass M_N) according to our convention for G_{MB}^*.

3.1.4. Parametrization of the quark current. To parameterize the quark current given by equation (3.6), we adopt the structure inspired by the vector meson dominance (VMD) mechanism as in [20, 31],

$$\begin{aligned}
f_{1\pm} &= \lambda_q + (1-\lambda_q)\frac{m_\rho^2}{m_\rho^2+Q^2} + c_\pm \frac{M_h^2 Q^2}{(M_h^2+Q^2)^2},\\
f_{10} &= \lambda_q + (1-\lambda_q)\frac{m_\phi^2}{m_\phi^2+Q^2} + c_0 \frac{M_h^2 Q^2}{(M_h^2+Q^2)^2},\\
f_{2\pm} &= \kappa_\pm \left\{ d_\pm \frac{m_\rho^2}{m_\rho^2+Q^2} + (1-d_\pm)\frac{M_h^2}{M_h^2+Q^2} \right\},\\
f_{20} &= \kappa_s \left\{ d_0 \frac{m_\phi^2}{m_\phi^2+Q^2} + (1-d_0)\frac{M_h^2}{M_h^2+Q^2} \right\},
\end{aligned} \tag{3.15}$$

where m_ρ, m_ϕ and M_h are the masses respectively corresponding to the light vector meson (ρ meson), the ϕ meson (associated with an $s\bar{s}$ state), and an effective heavy meson with mass $M_h = 2M_N$ to represent the short-range phenomenology. We use the mass value m_ρ for both isoscalar (corresponding ω meson) and isovector channels since $m_\omega \simeq m_\rho$. The coefficients $c_0, c_\pm$ and $d_0, d_\pm$ were determined in the previous studies for nucleon (model II) [20] and Ω^- [31]. The values are, respectively, $c_+ = 4.160$, $c_- = 1.160$, $d_+ = d_- = -0.686$, $c_0 = 4.427$ and $d_0 = -1.860$ [31]. The constant $\lambda_q = 1.21$ is obtained so as to reproduce correctly the quark number density in deep inelastic scattering [20].

The quark form factors parameterized by the VMD mechanism in equation (3.15) are particularly convenient to extend the model to other regimes besides the physical regime, because the quark current is written in terms of the vector meson and nucleon masses. In the previous work the model was extended successfully to the lattice QCD regime replacing these masses by those of the lattice regime [27]. Furthermore, the model was also applied to the lattice regime for the nucleon [35], $\gamma N \to \Delta$ reaction [34, 35], and octet and decuplet baryons [27, 31].

3.1.5. Scalar wavefunctions. The scalar wavefunctions are given by [27],

$$\psi_N(P,k) = \frac{N_N}{m_D(\beta_1+\chi_{_N})(\beta_2+\chi_{_N})}, \tag{3.16}$$

$$\psi_\Lambda(P,k) = \frac{N_\Lambda}{m_D(\beta_1+\chi_{_\Lambda})(\beta_3+\chi_{_\Lambda})}, \tag{3.17}$$

$$\psi_\Sigma(P,k) = \frac{N_\Sigma}{m_D(\beta_1+\chi_{_\Sigma})(\beta_3+\chi_{_\Sigma})}, \tag{3.18}$$

$$\psi_\Xi(P,k) = \frac{N_\Xi}{m_D(\beta_1+\chi_{_\Xi})(\beta_4+\chi_{_\Xi})}, \tag{3.19}$$

where N_B $(B = N, \Lambda, \Sigma, \Xi)$ are the normalization constants, and

$$\chi_{_B} = \frac{(M_B - m_D)^2 - (P-k)^2}{M_B m_D}. \tag{3.20}$$

Note that, except for the masses, the Λ and Σ scalar wavefunctions are the same. The normalization constants N_B are determined by

$$\int_k |\psi_B(\bar{P},k)|^2 = 1, \tag{3.21}$$

where $\bar{P} = (M_B, 0, 0, 0)$ is the baryon four-momentum at its rest frame.

In equations (3.16)-(3.19) the parameters β_i $(i = 1, .., 4)$ define the momentum range in units of m_D. The parameter β_1 is associated with the long-range scale (low-momentum range) that is common to all the octet baryon members. As for the remaining parameters $\beta_2, \beta_3, \beta_4 > \beta_1$, they are associated with the shorter range scale (larger momentum range). Namely, β_2 defines the short-range scale for the systems with only light quarks u and d, β_3 defines the short-range scale for the systems with one strange quark, and β_4 defines the scale for the systems with two strange quarks. As the strange quarks are heavier than the u and d quarks, and therefore more confined in the space, we expect that $\beta_2 > \beta_3 > \beta_4$. The parameters β_i $(i = 1, .., 4)$ as well as κ_u, κ_d will be fixed later.

3.2. Pion cloud dressing

We discuss here the pion cloud contributions for the electromagnetic current and form factors represented by the diagrams in figure 1. Following [26], we assume the pion as the dominant meson excitation to be included in the octet baryon form factors. Then, the meson cloud contributions for the octet baryon electromagnetic form factors can be described in terms of 6 independent functions of Q^2, related to the pion-baryon Feynman integral as will be described next.

3.2.1. Pion cloud electromagnetic currents. The pion cloud corrections, namely the coupling of the photon to the pion J^μ_π, and the coupling to the intermediate baryons $J^\mu_{\gamma B}$, defined by equation (3.1), can be written [26, 27]

$$J^\mu_\pi = \left(\tilde{B}_1\gamma^\mu + \tilde{B}_2\frac{i\sigma^{\mu\nu}q_\nu}{2M_B}\right)G_{\pi B}, \tag{3.22}$$

$$J^\mu_{\gamma B} = \left(\tilde{C}_1\gamma^\mu + \tilde{C}_2\frac{i\sigma^{\mu\nu}q_\nu}{2M_B}\right)G_{eB} + \left(\tilde{D}_1\gamma^\mu + \tilde{D}_2\frac{i\sigma^{\mu\nu}q_\nu}{2M_B}\right)G_{\kappa B}. \tag{3.23}$$

In the above, $\tilde{B}_i$, $\tilde{C}_i$ and $\tilde{D}_i$ $(i = 1, 2)$ are functions of Q^2 and $G_{\pi B}$, G_{eB}, $G_{\kappa B}$ are coefficients that depend on the baryon species $(B = N, \Sigma, \Lambda, \Xi)$. We assume that the functions $\tilde{B}_i$, $\tilde{C}_i$ and $\tilde{D}_i$ are only weakly dependent on the baryon masses, and the same for all the octet baryons as in [26]. That allows a description of the pion cloud dressing with a reduced number of coefficients. We write B_i, C_i, and D_i to represent respectively the functions $\tilde{B}_i$, $\tilde{C}_i$ and $\tilde{D}_i$ at $Q^2 = 0$.

The coefficients $G_{\pi B}$, G_{eB}, $G_{\kappa B}$ include the dependence on the pion-baryon coupling constants. According to $SU(3)$ symmetry [59, 60] the coupling constant of the pion (π) and baryons (B and B'), $g_{\pi BB'}$, can be represented in terms of the ratio, $\alpha = \frac{D}{F+D}$ and a global coupling constant $g = g_{\pi NN}$, the πNN coupling constant. We can then express $G_{\pi B}$, G_{eB}, $G_{\kappa B}$ in terms of the parameter α and a global factor g^2. For convenience we absorb the factor g^2 in the functions $\tilde{B}_i, \tilde{C}_i$ and $\tilde{D}_i$ $(i = 1, 2)$ and represent the effect of the coupling in terms of 4 independent constants [26, 27] associated with the octet baryon species‡,

$$\beta_N = 1, \tag{3.24}$$

$$\beta_\Lambda = \frac{4}{3}\alpha^2, \tag{3.25}$$

$$\beta_\Sigma = 4(1-\alpha)^2, \tag{3.26}$$

$$\beta_\Xi = (1-2\alpha)^2. \tag{3.27}$$

These constants encapsulate the effect of the coupling constants. The explicit dependence of $G_{\pi B}$, G_{eB} and $G_{\kappa B}$ on the constants given by equations (3.24)-(3.27) and on the bare form factors $\tilde{e}_{0B}$ and $\tilde{\kappa}_{0B}$ was derived in [26, 27]. In the following we use the results of [27].

From the equations above, we get $\beta_N = 1$, $\beta_\Lambda = 0.48$, $\beta_\Sigma = 0.64$ and $\beta_\Xi = 0.04$ with $\alpha = 0.6$, determined in combination with an $SU(6)$ quark model. It is therefore expected that the pion cloud contributions are small for the Ξ system. In this case the kaon cloud contribution may be more significant.

3.2.2. Dressed form factors. The octet baryon dressed form factors associated with the current (3.1), are obtained by the contributions from the quark core given by equations (3.10)-(3.11), and the pion cloud dressing via equations (3.22)-(3.23):

$$\begin{aligned} J^\mu_B = {} & Z_B \left[\tilde{e}_{0B} + G_{\pi B}\tilde{B}_1 + G_{eB}\tilde{C}_1 + G_{\kappa B}\tilde{D}_1\right]\gamma^\mu + \\ & Z_B \left[\tilde{\kappa}_{0B} + G_{\pi B}\tilde{B}_2 + G_{eB}\tilde{C}_2 + G_{\kappa B}\tilde{D}_2\right]\frac{i\sigma^{\mu\nu}q_\nu}{2M_B}. \end{aligned} \tag{3.28}$$

Using the above expressions and the definition of the form factors (2.1), we can write down the final results for the form factors F_{1B} and F_{2B}:

$$F_{1p} = Z_N\left\{\tilde{e}_{0p} + 2\beta_N\tilde{B}_1 + \beta_N(\tilde{e}_{0p} + 2\tilde{e}_{0n})\tilde{C}_1 + \beta_N(\tilde{\kappa}_{0p} + 2\tilde{\kappa}_{0n})\tilde{D}_1\right\}, \tag{3.29}$$

$$F_{1n} = Z_N\left\{\tilde{e}_{0n} - 2\beta_N\tilde{B}_1 + \beta_N(2\tilde{e}_{0p} + \tilde{e}_{0n})\tilde{C}_1 + \beta_N(2\tilde{\kappa}_{0p} + \tilde{\kappa}_{0n})\tilde{D}_1\right\}, \tag{3.30}$$

$$F_{1\Lambda} = Z_\Lambda\left\{\tilde{e}_{0\Lambda} + \beta_\Lambda(\tilde{e}_{0\Sigma^+} + \tilde{e}_{0\Sigma^0} + \tilde{e}_{0\Sigma^-})\tilde{C}_1 + \beta_\Lambda(\tilde{\kappa}_{0\Sigma^+} + \tilde{\kappa}_{0\Sigma^0} + \tilde{\kappa}_{0\Sigma^-})\tilde{D}_1\right\},$$

‡ The coefficient β_N was not considered explicitly in the previous works [26, 27], where $\beta_N \equiv 1$, but it is included here for completeness and to clarify the extension of the model to the in-medium case.

(3.31)

$$F_{1\Sigma^+} = Z_\Sigma \Big\{ \tilde{e}_{0\Sigma^+} + (\beta_\Sigma + \beta_\Lambda)\tilde{B}_1 + [\beta_\Sigma(\tilde{e}_{0\Sigma^+} + \tilde{e}_{0\Sigma^0}) + \beta_\Lambda \tilde{e}_{0\Lambda}]\,\tilde{C}_1 + [\beta_\Sigma(\tilde{\kappa}_{0\Sigma^+} + \tilde{\kappa}_{0\Sigma^0}) + \beta_\Lambda \tilde{\kappa}_{0\Lambda}]\,\tilde{D}_1 \Big\}, \tag{3.32}$$

$$F_{1\Sigma^0} = Z_\Sigma \Big\{ \tilde{e}_{0\Sigma^0} + [\beta_\Sigma(\tilde{e}_{0\Sigma^+} + \tilde{e}_{0\Sigma^-}) + \beta_\Lambda \tilde{e}_{0\Lambda}]\,\tilde{C}_1 + [\beta_\Sigma(\tilde{\kappa}_{0\Sigma^+} + \tilde{\kappa}_{0\Sigma^-}) + \beta_\Lambda \tilde{\kappa}_{0\Lambda}]\,\tilde{D}_1 \Big\}, \tag{3.33}$$

$$F_{1\Sigma^-} = Z_\Sigma \Big\{ \tilde{e}_{0\Sigma^-} - (\beta_\Sigma + \beta_\Lambda)\tilde{B}_1 + [\beta_\Sigma(\tilde{e}_{0\Sigma^0} + \tilde{e}_{0\Sigma^-}) + \beta_\Lambda \tilde{e}_{0\Lambda}]\,\tilde{C}_1 + [\beta_\Sigma(\tilde{\kappa}_{0\Sigma^0} + \tilde{\kappa}_{0\Sigma^-}) + \beta_\Lambda \tilde{\kappa}_{0\Lambda}]\,\tilde{D}_1 \Big\}, \tag{3.34}$$

$$F_{1\Xi^0} = Z_\Sigma \Big\{ \tilde{e}_{0\Xi^0} + 2\beta_\Xi \tilde{B}_1 + \beta_\Xi(\tilde{e}_{0\Xi^0} + 2\tilde{e}_{0\Xi^-})\tilde{C}_1 + \beta_\Xi(\tilde{\kappa}_{0\Xi^0} + 2\tilde{\kappa}_{0\Xi^-})\tilde{D}_1 \Big\}, \tag{3.35}$$

$$F_{1\Xi^-} = Z_\Sigma \Big\{ \tilde{e}_{0\Xi^-} - 2\beta_\Xi \tilde{B}_1 + \beta_\Xi(2\tilde{e}_{0\Xi^0} + \tilde{e}_{0\Xi^-})\tilde{C}_1 + \beta_\Xi(2\tilde{\kappa}_{0\Xi^0} + \tilde{\kappa}_{0\Xi^-})\tilde{D}_1 \Big\}, \tag{3.36}$$

$$F_{2p} = Z_N \Big\{ \tilde{\kappa}_{0p} + 2\beta_N \tilde{B}_2 + \beta_N(\tilde{e}_{0p} + 2\tilde{e}_{0n})\tilde{C}_2 + \beta_N(\tilde{\kappa}_{0p} + 2\tilde{\kappa}_{0n})\tilde{D}_2 \Big\}, \tag{3.37}$$

$$F_{2n} = Z_N \Big\{ \tilde{\kappa}_{0n} - 2\beta_N \tilde{B}_2 + \beta_N(2\tilde{e}_{0p} + \tilde{e}_{0n})\tilde{C}_2 + \beta_N(2\tilde{\kappa}_{0p} + \tilde{\kappa}_{0n})\tilde{D}_2 \Big\}, \tag{3.38}$$

$$F_{2\Lambda} = Z_\Lambda \Big\{ \tilde{\kappa}_{0\Lambda} + \beta_\Lambda(\tilde{e}_{0\Sigma^+} + \tilde{e}_{0\Sigma^0} + \tilde{e}_{0\Sigma^-})\tilde{C}_2 + \beta_\Lambda(\tilde{\kappa}_{0\Sigma^+} + \tilde{\kappa}_{0\Sigma^0} + \tilde{\kappa}_{0\Sigma^-})\tilde{D}_2 \Big\}, \tag{3.39}$$

$$F_{2\Sigma^+} = Z_\Sigma \Big\{ \tilde{\kappa}_{0\Sigma^+} + (\beta_\Sigma + \beta_\Lambda)\tilde{B}_2 + [\beta_\Sigma(\tilde{e}_{0\Sigma^+} + \tilde{e}_{0\Sigma^0}) + \beta_\Lambda \tilde{e}_{0\Lambda}]\,\tilde{C}_2 + [\beta_\Sigma(\tilde{\kappa}_{0\Sigma^+} + \tilde{\kappa}_{0\Sigma^0}) + \beta_\Lambda \tilde{\kappa}_{0\Lambda}]\,\tilde{D}_2 \Big\}, \tag{3.40}$$

$$F_{2\Sigma^0} = Z_\Sigma \Big\{ \tilde{\kappa}_{0\Sigma^0} + [\beta_\Sigma(\tilde{e}_{0\Sigma^+} + \tilde{e}_{0\Sigma^-}) + \beta_\Lambda \tilde{e}_{0\Lambda}]\,\tilde{C}_2 + [\beta_\Sigma(\tilde{\kappa}_{0\Sigma^+} + \tilde{\kappa}_{0\Sigma^-}) + \beta_\Lambda \tilde{\kappa}_{0\Lambda}]\,\tilde{D}_2 \Big\}, \tag{3.41}$$

$$F_{2\Sigma^-} = Z_\Sigma \Big\{ \tilde{\kappa}_{0\Sigma^-} - (\beta_\Sigma + \beta_\Lambda)\tilde{B}_2 + [\beta_\Sigma(\tilde{e}_{0\Sigma^0} + \tilde{e}_{0\Sigma^-}) + \beta_\Lambda \tilde{e}_{0\Lambda}]\,\tilde{C}_2 + [\beta_\Sigma(\tilde{\kappa}_{0\Sigma^0} + \tilde{\kappa}_{0\Sigma^-}) + \beta_\Lambda \tilde{\kappa}_{0\Lambda}]\,\tilde{D}_2 \Big\}, \tag{3.42}$$

$$F_{2\Xi^0} = Z_\Sigma \Big\{ \tilde{\kappa}_{0\Xi^0} + 2\beta_\Xi \tilde{B}_2 + \beta_\Xi(\tilde{e}_{0\Xi^0} + 2\tilde{e}_{0\Xi^-})\tilde{C}_2 + \beta_\Xi(\tilde{\kappa}_{0\Xi^0} + 2\tilde{\kappa}_{0\Xi^-})\tilde{D}_2 \Big\}, \tag{3.43}$$

$$F_{2\Xi^-} = Z_\Sigma \Big\{ \tilde{\kappa}_{0\Xi^-} - 2\beta_\Xi \tilde{B}_2 + \beta_\Xi(2\tilde{e}_{0\Xi^0} + \tilde{e}_{0\Xi^-})\tilde{C}_2 + \beta_\Xi(2\tilde{\kappa}_{0\Xi^0} + \tilde{\kappa}_{0\Xi^-})\tilde{D}_2 \Big\}. \tag{3.44}$$

The normalization constants are

$$\begin{aligned} Z_N &= \left[1 + 3\beta_N B_1\right]^{-1} \\ Z_\Lambda &= \left[1 + 3\beta_\Lambda B_1\right]^{-1}, \\ Z_\Sigma &= \left[1 + \left(2\beta_\Sigma + \beta_\Lambda\right) B_1\right]^{-1}, \\ Z_\Xi &= \left[1 + 3\beta_\Xi B_1\right]^{-1}, \end{aligned} \tag{3.45}$$

and we refer to [26, 27] for more details.

Using the above expressions, one can calculate the electric and magnetic form factors both in vacuum, based on equations (2.3) and (2.4), and in medium based on equations (2.7)-(2.8).

From the discussions in the previous sections, the baryon form factors F_{iB} $(i = 1, 2)$ may be decomposed into

$$F_{iB}(Q^2) = Z_B \left[F_{i0B}(Q^2) + \delta F_{iB}(Q^2)\right], \tag{3.46}$$

where F_{10B} and F_{20B} are defined by equation (3.4), and the corresponding pion cloud contributions δF_{1B} and δF_{2B} are given in equations (3.29)-(3.44). It is natural to regard $Z_B F_{i0B}$ as representing the valence quark effects and $Z_B \delta F_{iB}$ those of the pion cloud.

The same decomposition can be applied for the electric and magnetic form factors:

$$\begin{aligned} G_{EB}(Q^2) &= Z_B \left[G_{E0B}(Q^2) + \delta G_{EB}(Q^2)\right], \\ G_{MB}(Q^2) &= Z_B \left[G_{M0B}(Q^2) + \delta G_{MB}(Q^2)\right], \end{aligned} \tag{3.47}$$

where G_{E0B}, G_{M0B} are defined by equations (3.13) and (3.14), and $\delta G_{EB} = \delta F_{1B} - \tau \delta F_{2B}$ and $\delta G_{MB} = [\delta F_{1B} + \delta F_{2B}] \frac{M_N}{M_B}$. In this case $Z_B \delta G_{EB}$, and $Z_B \delta G_{MB}$ reflect the dressing of the pion cloud. To estimate the pion cloud contributions, we compare the full result, G_{EB} or G_{MB}, with the total contributions of the valence quark core, $Z_B G_{E0B}$ or $Z_B G_{M0B}$. The difference is the pion cloud contributions, $Z_B \delta G_{EB}$ or $Z_B \delta G_{MB}$.

4. Including chiral symmetry in the pion cloud parametrization

The effect of chiral symmetry in the electromagnetic structure of the octet baryons can be analyzed by studying the dependence of the form factors on m_π and the corresponding behavior in the chiral limit ($m_\pi \to 0$). In the chiral limit the pion cloud extends to infinity, leading to the divergence of the nucleon radius.

In this section we start reviewing the main features of the chiral behavior for the nucleon radii. At this stage we do not attempt to describe the nucleon magnetic moments including the pion mass dependence, since the dependence is milder than that for the nucleon radii [61, 62, 63]. Next, we derive the general expressions for the nucleon radii in the present model. Finally, we present the newly updated parametrization for the pion cloud contributions, and describe how the chiral behavior is implemented in the model.

Table 2. Nucleon radii. We adopt the average values from the PDG [67] more recent results. All values in fm^2. The Pauli isovector square radii normalized is $\frac{(r_2^V)^2}{\kappa_V} = 0.418 \pm 0.012$ fm^2.

r^2_{Ep}	r^2_{Mp}	r^2_{En}	r^2_{Mn}	$(r_1^V)^2$	$(r_2^V)^2$
0.7634±0.0140	0.6983±0.0109	−0.1161±0.0022	0.7430±0.0134	0.0634±0.0142	1.5509±0.0430

4.1. Nucleon radii in the chiral limit

The leading order effects of chiral symmetry can be better observed in the nucleon isovector form factor [64] defined by,

$$F_1^V(Q^2) = F_{1p}(Q^2) - F_{1n}(Q^2), \tag{4.1}$$

$$F_2^V(Q^2) = F_{2p}(Q^2) - F_{2n}(Q^2). \tag{4.2}$$

Using these decompositions we can define the isovector Dirac and Pauli square radii:

$$(r_1^V)^2 = -6\,\frac{dF_1^V}{dQ^2}\bigg|_{Q^2=0}, \tag{4.3}$$

$$(r_2^V)^2 = -6\,\frac{dF_2^V}{dQ^2}\bigg|_{Q^2=0}. \tag{4.4}$$

Note that in the definitions we do not normalize the respective radius at $Q^2 = 0$ as usually done. To compare $(r_2^V)^2$ with the experimental value the result must be divided by $\kappa_V = \kappa_p - \kappa_n \simeq 3.7$ (isovector anomalous magnetic moment).

We now discuss the expected result in the small pion mass limit. According to χPT [65, 66] the isovector square radii $(r_1^V)^2$ and $(r_2^V)^2$ can be expressed as

$$(r_1^V)^2 = -\frac{\alpha_1}{\alpha_0}\log m_\pi + A_1, \tag{4.5}$$

$$(r_2^V)^2 = +\frac{\alpha_2}{\alpha_0}\frac{M}{m_\pi} + A_2, \tag{4.6}$$

where m_π and M are the pion and nucleon masses, respectively, and

$$\alpha_0 = 8\pi^2 F_\pi^2, \tag{4.7}$$

$$\alpha_1 = 5g_A^2 + 1, \tag{4.8}$$

$$\alpha_2 = \pi g_A^2, \tag{4.9}$$

with $F_\pi = 93$ MeV and $g_A = 1.27$. In the above, A_1 and A_2 represent constant terms and higher powers of m_π^2, that can be expressed by constants at the physical point.

We take a pragmatic approach and fix these constant values using the experimental values of $(r_1^V)^2$ and $(r_2^V)^2$. The results obtained from the average values§ of the PDG results [67] are presented in table 2. From the table we find $A_1 \simeq 12.05$ fm^2 and $A_2 \simeq -38.20$ fm^2. These results are obtained assuming the physical value of m_π and the experimental results.

§ For the neutron radii r^2_{En} and r^2_{Mn} we use the results suggested by PDG [67]. For the proton radii there is still controversy. For r^2_{Mp} we take the arithmetic average of the 3 results listed. As for r^2_{Ep} we simply take the arithmetic average of the first 12 results from the list (since 2000), irrespective of the different types of the determinations, electronic, muonic, or others.

4.2. Isovector form factors and respective radii

We discuss now the isovector form factors given by the present model.

Using equations (3.29)-(3.30) and (3.37)-(3.38) we can write

$$F_1^V(Q^2) = Z_N \left\{ (\tilde{e}_{0p} - \tilde{e}_{0n}) + 4\tilde{B}_1 - (\tilde{e}_{0p} - \tilde{e}_{0n})\tilde{C}_1 - (\tilde{\kappa}_{0p} - \tilde{\kappa}_{0n})\tilde{D}_1 \right\} \quad (4.10)$$

$$F_2^V(Q^2) = Z_N \left\{ (\tilde{\kappa}_{0p} - \tilde{\kappa}_{0n}) + 4\tilde{B}_2 - (\tilde{e}_{0p} - \tilde{e}_{0n})\tilde{C}_2 - (\tilde{\kappa}_{0p} - \tilde{\kappa}_{0n})\tilde{D}_2 \right\} \quad (4.11)$$

From these equations we conclude that the nucleon isovector form factors are given by the difference between the proton and neutron bare form factors ($\tilde{e}_{0N}$ or $\tilde{\kappa}_{0N}$) and the pion cloud contributions.

The results for the isovector square radii are given by

$$(r_1^V)^2 = Z_N \left\{ -24 \left. \frac{d\tilde{B}_1}{dQ^2} \right|_0 + R_1 \right\}, \quad (4.12)$$

$$(r_2^V)^2 = Z_N \left\{ -24 \left. \frac{d\tilde{B}_2}{dQ^2} \right|_0 + R_2 \right\}, \quad (4.13)$$

where

$$R_1 = 6 \left. \frac{d\tilde{C}_1}{dQ^2} \right|_0 + (1 - C_1)(r_{10p}^2 - r_{10n}^2) + 6(\kappa_{0p} - \kappa_{0n}) \left. \frac{d\tilde{D}_1}{dQ^2} \right|_0, \quad (4.14)$$

$$R_2 = 6 \left. \frac{d\tilde{C}_2}{dQ^2} \right|_0 - (r_{10p}^2 - r_{10n}^2)C_2 + (1 - D_2)(r_{20p}^2 - r_{20n}^2) + 6(\kappa_{0p} - \kappa_{0n}) \left. \frac{d\tilde{D}_2}{dQ^2} \right|_0. \quad (4.15)$$

In the above expressions $|_0$ stands for the derivative at $Q^2 = 0$, and

$$r_{i0B}^2 = -6 \left. \frac{dF_{i0B}}{dQ^2} \right|_{Q^2=0} (i = 1, 2), \quad (4.16)$$

represent the *bare* radii.

The expressions (4.12) and (4.13) are still general. We now discuss the constraints of chiral perturbation theory for the model.

4.3. Pion cloud parametrization

We consider the following parametrizations for the functions $\tilde{B}_1$ and $\tilde{B}_2$:

$$\tilde{B}_1 = B_1 \left(\frac{\Lambda_1^2}{\Lambda_1^2 + Q^2} \right)^5 \left[1 + \frac{1}{Z_N B_1} \left(\frac{1}{24} \frac{\alpha_1}{\alpha_0} \log m_\pi + b_1' \right) Q^2 \right], \quad (4.17)$$

$$\tilde{B}_2 = B_2 \left(\frac{\Lambda_2^2}{\Lambda_2^2 + Q^2} \right)^6 \left[1 + \frac{1}{Z_N B_2} \left(-\frac{1}{24} \frac{\alpha_2}{\alpha_0} \frac{M}{m_\pi} + b_2' \right) Q^2 \right]. \quad (4.18)$$

Here B_1 and B_2 are constants given respectively by $\tilde{B}_1(0)$ and $\tilde{B}_2(0)$, and Λ_1, Λ_2 are two cutoffs to be fixed by a fit to the data.

As for b_1' and b_2' they are two additional parameters that will be fixed by the experimental results for the nucleon isovector square radii, equations (4.5) and (4.6).

Inserting the above expressions into equations (4.12) and (4.13) we can write

$$(r_1^V)^2 = -\frac{\alpha_1}{\alpha_0}\log m_\pi + Z_N\left\{-24\frac{b_1'}{Z_N} - 120\frac{B_1}{\Lambda_1^2} + R_1\right\}, \tag{4.19}$$

$$(r_2^V)^2 = +\frac{\alpha_2}{\alpha_0}\frac{M}{m_\pi} + Z_N\left\{-24\frac{b_2'}{Z_N} - 144\frac{B_1}{\Lambda_1^2} + R_2\right\}. \tag{4.20}$$

Note that the second term in each equation above should be identified with A_1 and A_2 in equations (4.5) and (4.6), respectively.

As for the remaining functions we use

$$\tilde{C}_1 = B_1\left(\frac{\Lambda_1^2}{\Lambda_1^2+Q^2}\right)^2, \tag{4.21}$$

$$\tilde{D}_1 = D_1'\frac{Q^2\Lambda_1^4}{(\Lambda_1^2+Q^2)^3}, \tag{4.22}$$

$$\tilde{C}_2 = C_2\left(\frac{\Lambda_2^2}{\Lambda_2^2+Q^2}\right)^3, \tag{4.23}$$

$$\tilde{D}_2 = D_2\left(\frac{\Lambda_2^2}{\Lambda_2^2+Q^2}\right)^3. \tag{4.24}$$

Again C_2 and D_2 are the constants given by the value at $Q^2 = 0$ for the respective functions. D_1' is a new constant defined by $D_1' = \frac{1}{\Lambda_1^2}\frac{dD_1}{dQ^2}(0)$. Note that $\tilde{C}_1(0) = B_1$, a constraint required by the conditions $F_{1p}(0) = 1$ and $F_{1n}(0) = 0$ (nucleon charges) [26, 27]. The definition of $\tilde{D}_1$ that vanishes at $Q^2 = 0$ is also motivated by the nucleon charge conditions. The parametrizations used for $\tilde{C}_1, \tilde{D}_1, \tilde{C}_2$ and $\tilde{D}_2$ are the same as those presented in [27]. The leading order chiral effects in the form factors in the present parametrization come exclusively from $\tilde{B}_1$ and $\tilde{B}_2$. We choose to use the same cutoffs in C_i, D_i as those used in B_i (Λ_1 and Λ_2, for the Dirac and Pauli form factors) in order to reduce the number of parameters in the model [27].

Finally, we can now write down,

$$R_1 = -12\frac{B_1}{\Lambda_1^2} + (1-C_1)(r_{10p}^2 - r_{10n}^2) + 6(\kappa_{0p}-\kappa_{0n})\frac{D_1'}{\Lambda_1^2}, \tag{4.25}$$

$$R_2 = -18\frac{C_2}{\Lambda_2^2} + (1-D_2)(r_{20p}^2 - r_{20n}^2) - (r_{10p}^2 - r_{10n}^2)C_2 - 18(\kappa_{0p}-\kappa_{0n})\frac{D_2}{\Lambda_2^2}. \tag{4.26}$$

The values of the coefficients b_1' and b_2' can now be determined comparing equations (4.19) and (4.20) with equations (4.5) and (4.6).

The choice of the powers included in the pion cloud functions is phenomenological and motivated by the expected falloff of the quark-antiquark contributions in the large Q^2 limit [68] as well as the magnitude of the pion cloud contributions estimated for the $\gamma N \to \Delta$ reaction [24, 33, 34]. With the present parametrization the pion cloud contributions fall off by a factor $1/Q^4$ faster than the falloff of the valence quark contributions.

5. Extension of the spectator quark model to the in-medium regime

We now discuss the extension of the model for the in-medium regime. In general we consider the modifications of the model due to the in-medium environment. As for the valence quark core part, the in-medium hadron masses appearing in the model, M_B ($B = N, \Lambda, \Sigma, \Xi$), m_ρ, m_ϕ and M_h, will be respectively denoted by M_B^* ($B = N, \Lambda, \Sigma, \Xi$), m_ρ^*, m_ϕ^* and M_h^* (given by $2M_N^*$). On the other hand, for the pion cloud effects we consider the modifications of the pion-baryon couplings in the in-medium regime as will be explained next. In this study we do not include any final state interactions nor meson exchange current, as mentioned in introduction.

5.1. In-medium regime: quark core

Although lattice QCD simulation has been very rapidly developing recently, it is still very difficult to study the properties of hadrons in finite nucleon (baryon) densities near and higher than the normal nuclear matter densities. Thus, we need to resort to some phenomenological models which have proven successful in studying nuclear phenomena and nuclear processes based on the quark degrees of freedom. For this purpose, we use the quark-meson coupling (QMC) model [39, 40], which has been successfully applied to study the properties of baryons and mesons in nuclei and nuclear medium.

We note that, combined with the cloudy bag model (CBM) [69], QMC had indeed predicted [10] an in-medium modification of the bound proton electromagnetic form factors which turned out to be consistent with the experimentally observed modification [4, 5, 6, 7]. Below, we use a different model, the covariant spectator quark model [20, 23, 24], which was successfully applied to study the octet baryon electromagnetic form factors [27] utilizing the lattice QCD simulation data. By the use of different models, we hope to shed light on the mechanism of the in-medium modification of the bound proton electromagnetic form factors. Furthermore, we predict in-medium electromagnetic form factors of all members of the octet baryons.

The current j_q^μ, given by equation (3.6), is also characterized by the corresponding in-medium masses in terms of the two components j_1 and j_2, which are represented based on the VMD parametrization in equations (3.15).

In the quark current (3.6), we replace the coefficient of the Pauli form factor $1/(2M_N)$ by $1/(2M_N^*)$ in the in-medium regime. As for the quark form factors, we use equation (3.15) with the meson masses replaced by the respective in-medium masses similarly to the lattice regime studies [27, 31, 34, 35]. That is, we replace m_ρ and m_ϕ by the in-medium ρ mass m_ρ^*, and ϕ mass m_ϕ^*, and the effective heavy meson mass of $M_h = 2M_N$ by $2M_N^*$.

As for the wavefunctions Ψ_B, M_B is replaced by M_B^* in medium. This applies for the radial (scalar) wavefunctions (3.16)-(3.19). As explained the scalar wavefunctions for the octet baryons are represented in terms of four independent momentum range parameters β_i ($i = 1, .., 4$). We assume that these parameters are independent of the baryon masses in vacuum, and therefore also independent of the in-medium baryon masses. There is no need to modify the diquark mass in in medium, since the electromagnetic form factors are independent of it [20, 27]. For the in-medium regime the pion mass m_π^*, which is relevant for the present study, it was estimated in [72] that $m_\pi^* \simeq m_\pi$ at normal nuclear matter density (0.15 fm^{-3}). Thus, we use the vacuum value, $m_\pi = 138.0$ MeV for the densities considered in this study. The in-medium hadron masses mostly calculated in QMC, and the relevant values for the

Table 3. Hadron masses (in MeV) necessary for the in-medium regime of the model with $\rho_0 = 0.15$ fm^{-3}. For the vacuum case ($\rho = 0$) we take m_ρ as the average of ρ and ω masses as originally used in the model [20, 27].

	$\rho = 0$	$\rho = 0.5\,\rho_0$	$\rho = \rho_0$
M_N	939.0	831.3	754.5
M_Λ	1116.0	1043.9	992.7
M_Σ	1192.0	1121.4	1070.4
M_Ξ	1318.0	1282.2	1256.7
m_ρ	779.0	706.1	653.7
m_ϕ	1019.5	1019.1	1018.9
m_π	138.0	138.0	138.0

calculation, are listed in table 3.

Using the model extended to the in-medium regime, namely, using the quark currents and baryon wavefunctions for the in-medium regime, we can calculate the form factors G^*_{EB} and G^*_{MB} in a nuclear medium by the expressions given in section 3.1, for a model with no pion cloud dressing with the in-medium masses calculated in QMC for a given nuclear density.

5.2. In-medium regime: pion cloud

To extend the pion cloud effects of the model to the in-medium regime, we need other ingredients. Although we do not have a good control, we estimate the effects of the pion cloud in the nuclear medium. Thus, the estimates of the pion cloud effects in the nuclear medium presented below, should be taken in caution. Main task for this is to calculate the modifications of the baryon-pion coupling constants in medium, $g^*_{\pi BB'}$ ($B, B' = N, \Lambda, \Sigma, \Xi$). [As before, we denote the properties in the nuclear medium by asterisk *.] For the moment, we consider below the πBB diagonal case, and omit the $\pi\Lambda\Sigma$ coupling which appear in the pion cloud effects in the Λ and Σ cases containing the $g_{\pi\Lambda\Sigma}$ coupling from the discussion, but the procedure can be extended to also for the $\pi\Lambda\Sigma$ case. We assume that the pion cloud parametrization functions given by equations (4.17)-(4.18) and (4.21)-(4.24) defined in vacuum, are unmodified in the medium, since the pion mass in vacuum is used.

Our estimates of the in-medium couplings, $g^*_{\pi BB}$, relative to those in vacuum $g_{\pi BB}$ [69, 70], rely on the Goldberger-Treimann relation [71]. The in-medium to the free coupling constant ratio may be expressed by,

$$\begin{aligned} \frac{g^*_{\pi BB}}{g_{\pi BB}} &= \left(\frac{f_\pi}{f^*_\pi}\right)\left(\frac{g^{B*}_A}{g^B_A}\right)\left(\frac{M^*_B}{M_B}\right), \\ &\simeq \left(\frac{f_\pi}{f^*_\pi}\right)\left(\frac{g^{N*}_A}{g^N_A}\right)\left(\frac{M^*_B}{M_B}\right), \end{aligned} \tag{5.1}$$

where f_π, g^B_A and M_B are respectively the pion decay constant, axial coupling constant of the baryon B and its mass, and the corresponding quantities in nuclear matter with *. First for f^*_π, it was estimated in [72] and we use the $f^{(t)}_\pi$ in nuclear matter as f^*_π above. On the other hand, g^{N*}_A/g^N_A was estimated in QMC [73], and M^*_B/M_B as in table 3. For $g^*_{\pi\Lambda\Sigma}$, the relevant quantities different from the diagonal cases are M^*_Λ/M_Λ or M^*_Σ/M_Σ. To estimate the maximally modified case, we use M^*_Λ/M_Λ, although the

	$\rho = 0$	$\rho = 0.5\,\rho_0$	$\rho = \rho_0$
$g^*_{\pi NN}/g_{\pi NN}$	1	0.921	0.899
$g^*_{\pi\Lambda\Sigma}/g_{\pi\Lambda\Sigma}$	1	0.973	0.996
$g^*_{\pi\Sigma\Sigma}/g_{\pi\Sigma\Sigma}$	1	0.977	1.004
$g^*_{\pi\Xi\Xi}/g_{\pi\Xi\Xi}$	1	1.012	1.067

Table 4. Modification of the $\pi BB'$ coupling constants in nuclear matter with $\rho_0 = 0.15$ fm^{-3}.

difference is less than 1%. The modification of the coupling constants for the densities $\rho = 0.5\,\rho_0$ and ρ_0 are summarized in table 4. In table 4 the in-medium coupling constants $g^*_{\pi BB'}$ via equation (5.1) either decrease, or remain close to the vacuum values. In QMC it is expected that the values slightly decrease in medium, since the coupling is the same as that of the weak axial coupling constant g_A, namely $\gamma^\mu\gamma_5$ to the Dirac spinor, and g_A^{N*} in nuclear matter decreases [73]. Some unexpected behavior for $g^*_{\pi\Sigma\Sigma}$ and $g^*_{\pi\Xi\Xi}$ are due to the large decrease of f^*_π estimated in [72]. The decreasing rate of f^*_π in medium overcomes slightly that of the $g_A^{N*}M^*_\Sigma$ and $g_A^{N*}M^*_\Xi$, and thus $g^*_{\pi\Sigma\Sigma}$ and $g^*_{\pi\Xi\Xi}$ increase slightly. Thus, the trend of changing in values for $g^*_{\pi BB'}$ in nuclear matter, is consistent with that expected from QMC, although the latter generally does not contain the pion cloud effects, and it is this pion (f^*_π) which leads to slightly unexpected density dependence for $g^*_{\pi\Sigma\Sigma}$ and $g^*_{\pi\Xi\Xi}$.

Next, we comment on the effects of the baryon mass modifications in the intermediate baryon propagator in the nuclear medium. In the pion cloud dressing of the current shown in figure 1 in vacuum, the intermediate states baryons belong to the same isomultiplet except for the Λ and Σ cases. Therefore the intermediate baryon masses are the same or at most differ 1% (Λ and Σ). In-medium mass modifications of the baryons B' apply in the same way as those for the initial and final baryons, and thus the mass difference between the baryons B and B' in the nuclear medium is the same as those in vacuum, namely, $[M_{B'} - M_B] \simeq [M^*_{B'} - M^*_B]$, and we can approximately have the same pion cloud effects due to the modifications of the baryon masses. Thus, the modification of the pion cloud effects in the nuclear medium arises entirely from the modification of the pion-baryon coupling constants, $g^*_{\pi BB'}$, in the present approach.

Finally, we estimate the in-medium modifications for the pion cloud dressing by replacing the constants those in vacuum β_B ($B = N, \Lambda, \Sigma, \Xi$) given by equations (3.25)-(3.27), by the new constants β^*_B to be presented next. We keep the value $\alpha = 0.6$, the same as that in the vacuum, and use the in-medium coupling constants $g^*_{\pi BB'}$, and get β^*_B for $B = N, \Lambda, \Sigma, \Xi$,

$$\beta_N \to \beta^*_N = \left(\frac{g^*_{\pi NN}}{g_{\pi NN}}\right)^2, \tag{5.2}$$

$$\beta_\Lambda \to \beta^*_\Lambda = \frac{4}{3}\alpha^2\left(\frac{g^*_{\pi\Lambda\Sigma}}{g_{\pi\Lambda\Sigma}}\right)^2, \tag{5.3}$$

$$\beta_\Sigma \to \beta^*_\Sigma = 4(1-\alpha)^2\left(\frac{g^*_{\pi\Sigma\Sigma}}{g_{\pi\Sigma\Sigma}}\right)^2, \tag{5.4}$$

$$\beta_\Xi \to \beta^*_\Xi = (1-2\alpha)^2\left(\frac{g^*_{\pi\Xi\Xi}}{g_{\pi\Xi\Xi}}\right)^2. \tag{5.5}$$

Note that according to the relation between the constants β_B and the normalization constants Z_B [see equations (3.45)] the renormalization constants will also be modified to Z_B^* (replacing $\beta_B \to \beta_B^*$).

6. Results

According to the new constraints imposed on the model (chiral symmetry and fit to the experimental square radii) we readjust the parameters of the model and carry out a new calibration that differs from the one presented in [27].

We divide the presentation of our results in two parts. First, we will present the results of the new calibration for the vacuum, mainly concentrating on the nucleon form factors. Next, we will present the results for the baryon octet electromagnetic form factors in the nuclear medium, showing also each contribution from the valence quarks and pion cloud.

6.1. Octet baryon electromagnetic form factors in vacuum

We present here the results of the global fit in vacuum, and compare with the previous model in [27]. The values of the valence quark parameters including the momentum-range scales of the octet baryon wavefunctions and the u (κ_u) and d (κ_d) quark anomalous magnetic moments are presented in table 5. As for the parameters associated with the pion cloud, they are given in table 6.

We fit the parameters of the model to the nucleon data [74, 75, 76, 77, 78, 79, 80, 81, 82, 83, 84, 85, 86, 87], the octet lattice QCD data, the octet magnetic moments ($\Lambda, \Sigma^{+,-}, \Xi^{0,-}$) [67], the nucleon electric and magnetic radii and also the Σ^- electric radius. Following [27] we use some constraints in the fit to the octet lattice and physical data. The lattice data considered are the data with $m_\pi = 351, 591$ MeV from [88] for $n, p, \Sigma^{\pm}, \Xi^{0,-}$. For these pion mass values, the pion cloud effects are expected to be small.

To perform a fit we have taken care of the following points in order to achieve a fair description of *both* the physical and lattice data:

(i) The impact from the nucleon physical form factor data is doubled compared with the octet lattice form factor data.

(ii) Statistical errors are doubled for the neutral particles n and Ξ^0 to take into account the possible systematic errors in the lattice.

(iii) We double the error bars for the physical magnetic moment data to avoid dominating χ^2 due to the extremely accurate measurements in comparison with the nucleon physical form factor data.

(iv) The impact from the nucleon radii data are doubled to be consistent with the nucleon form factor data.

(v) The experimental error for the Σ^- electric square radius is reduced in our fit (from 0.15 fm^2 to 0.015 fm^2) in order to avoid the dominance of the nucleon square radii data in the fit and also to get the same order of contribution from the pion cloud as that for the proton.

Below we explain in detail the fitting procedure described above.

The first condition, the reinforcement of the impact of physical data in the fit is included since the number of physical data points (202) is inferior to the number

of lattice data points (272) as discussed in [27]. The reduction of the impact of the neutral particle lattice data was also discussed in detail in [27]. As for the magnetic moment data (magnetic form factors for $Q^2 = 0$) the fitting condition is included to avoid the excessive dominance of the $Q^2 = 0$ data. The first 3 conditions follow the procedure used in the previous work where the nucleon physical data and octet magnetic moments and the octet lattice data were used to calibrate the model [27]. We discuss now the inclusion of the data related with the electric and magnetic radii that explain the last two conditions.

As discussed, the available experimental information about the octet radii is restricted to the nucleon (p and n) electric and magnetic radii and the Σ^- electric radius. The nucleon square radii are given in table 2. For the Σ^- electric square radius the experimental value is $r^2_{E\Sigma^-} = 0.61 \pm 0.15$ fm^2 [89]. In the χ^2 calculation we use a factor 2 for the radii data to be consistent with the physical and lattice data in the χ^2 evaluation (impact 2, the same as the nucleon form factor data). The inclusion of the octet radii data is important to calibrate the low Q^2 regime of the model. In addition, the radii data constrain the degrees of freedom related to the pion cloud dressing, and reflect the effect of the chiral symmetry. Note however the large error associated with the Σ^- electric square radius. Although the nucleon radii data restrict the possible values to a small interval, the Σ^- electric square radius has a large interval of variation.

The minimization of the χ^2 using the result for the Σ^- electric square radius (with the error 0.15 fm^2) leads to a very large Σ^- electric square radius compared with that of the proton, as a consequence of much larger contribution from the pion cloud than that for the proton. A large pion cloud contribution for the Σ^- electric square radius contradicts what it is expected from $SU(3)$ symmetry, where the contribution is expected to be of comparable with that for the proton. Also, estimates of the pion cloud contribution from [48] for the electric square radii predict similar contributions for the proton and Σ^-. In order to impose a small pion cloud contribution to the Σ^- electric square radii with the amount close the the proton case, we reduce the error of Σ^- electric square radius in the χ^2 calculation to 0.015 fm^2 (instead of 0.15 fm^2). We consider then, for the Σ^- electric square radius an error bar comparable with the error bars from the nucleon radii. With the choice 0.015 fm^2, the contribution of the Σ^- electric radius to χ^2 is of the same order as the other contributions (particularly the proton magnetic square radius), and the calibration of the model is not dominated by a particular observable. An additional motivation to use a standard deviation for the Σ^- electric square radius with a magnitude ≈ 0.02 fm^2 is that we can achieve a simultaneous good description of the nucleon form factor data (χ^2 per data point ≈ 2) and lattice data (χ^2 per data point ≈ 6), as in the previous work, where the experimental information about the baryon radii was not taken into consideration [27]. We note that this is an *ad hoc* procedure, but in the absence of additional information about the quark core effect (or pion cloud) in the physical regime, it is the simplest way to make a realistic calibration of the present model. Later we will discuss the sensitivity of the final fit to the values of the $\Sigma^\pm$ electric radii.

From the parameters associated with the valence quark contributions in table 3.1, we note that $\beta_1 < \beta_2, \beta_3, \beta_4$ as expected from the interpretation of β_1, as the 3-quark long range parameter according to equations (3.16)-(3.19). Also the order of the momentum range scales $\beta_2 > \beta_3 > \beta_4$ are consistent with the fact that the system with only light quarks (parameter β_2) is more spread than a system with one strange quark (parameter β_3), and that it is less compact than a system with two strange

β_1	β_2	β_3	β_4
0.0532	0.809	0.603	0.381
	κ_u	κ_d	κ_s
	1.711	1.987	1.462

Table 5. Parameters associated with the valence quarks determined by the fit. The value of κ_s was determined in [31] in the study of the baryon decuplet. The analytical form of the scalar wavefunctions, depending on β_i $(i = 1, .., 4)$ are presented in section 3.1.

B_1, B_2	C_2	D_1', D_2	b_1', b_2'	Λ_1, Λ_2(GeV)
0.0510		-0.148	1.036	0.786
0.216	0.00286	0.0821	-1.987	1.132

Table 6. Parameters associated with the pion cloud dressing determined by the fit. See the parametrization of the functions $\tilde{B}_i, \tilde{C}_i$ and $\tilde{D}_i$ $(i = 1, 2)$ in section 3.2. The values of b_1', b_2' are calculated from the equations (4.5)-(4.6).

quarks (parameter β_4) in the position space. The same trend was *observed* in [27].

As for the values of the pion cloud parameters the more significant difference is the increase of B_1, which implies an increase of the pion cloud contribution for G_E, for the all members of the octet baryons, near $Q^2 = 0$. Taking the nucleon case as an example, $Z_N = 1/(1 + 3B_1) \simeq 0.87$ in the vacuum, means that the pion cloud contribution for the proton charge is about 13%. This is still rather small compared with a model such as CBM, yet in comparison with the previous work, the low Q^2 behavior of the functions $\tilde{B}_1$ and $\tilde{B}_2$ is modified. (See section 4.3). This modification changes significantly the behavior of the pion cloud parametrization. Nevertheless, the new parameter values are close to the previous ones except for C_2 [27], which is now much smaller (reduction in the effect of the Dirac form factors due to the process shown in figure 1(b) to the magnetic form factors).

Comparing the quality of the present fit with the previous one, we have obtained a slightly worse description of the lattice QCD data [χ^2 per data point of 6.0 to be compared with 5.0], and also a less accurate description of the nucleon data [χ^2 per data point of 1.99 to be compared with 1.93]. In detail we have now per data point,

$$\begin{aligned} &\chi^2(G_{Ep}) = 1.89, \quad \chi^2(G_{Mp}) = 1.69, \\ &\chi^2(G_{En}) = 1.78, \quad \chi^2(G_{Mn}) = 2.41, \end{aligned} \tag{6.1}$$

to be compared with the previous values of $\chi^2(G_{Ep}) = 1.60$, $\chi^2(G_{Mp}) = 1.87$, $\chi^2(G_{En}) = 1.86$ and $\chi^2(G_{Mn}) = 2.27$ [27]. In simple words we have improved the description of G_{En} but we have lost some precision in the description of the other form factors, particularly for G_{Mn}. The neutron magnetic form factor is difficult to describe as a consequence of the high accuracy of recent data, that disagree with the previous sets (see details in [27]). The loss of precision in some nucleon physical data is compensated by the quality of the description of the nucleon and Σ^- square radii, where the constraints from chiral symmetry are imposed.

The main electromagnetic properties of the octet baryons in vacuum, such as magnetic moments (in $\hat{\mu}_N$ units), the electric and magnetic square radii are presented in Table 7 and compared with the experimental results.

B	μ_B	μ_B^{exp}	r^2_{EB}	$(r^2_{EB})_{exp}$	r^2_{MB}	$(r^2_{MB})_{exp}$
p	2.737	2.793	0.782	0.763(14)	0.718	0.698(11)
n	-1.933	-1.913	-0.113	$-0.1161(22)$	0.729	0.743(13)
Λ	-0.628	-0.613(4)	0.068		0.228	
Σ^+	2.600	2.45(2)	0.713		0.516	
Σ^0	0.728		0.039		0.388	
Σ^-	-1.143	$-1.16(3)$	0.643	0.61(15)	0.642	
Ξ^0	-1.488	$-1.250(14)$	0.097		0.319	
Ξ^-	-0.689	$-0.65(3)$	0.403		0.268	

Table 7. Electromagnetic proprieties of octet baryons in vacuum. See Table 2 for the description of the nucleon radii data. Additional data are from [89] (Σ^- electric square radius) and [67] (magnetic moments).

The square radii are defined according to

$$r^2_{EB} = -\frac{6}{G_{EB}(0)}\frac{dG_{EB}}{dQ^2}\bigg|_{Q^2=0}, \tag{6.2}$$

$$r^2_{MB} = -\frac{6}{G_{MB}(0)}\frac{dG_{MB}}{dQ^2}\bigg|_{Q^2=0}. \tag{6.3}$$

Note that the square radii are normalized by the value of the form factor (G_{EB} or G_{MB}) at $Q^2 = 0$, the usual definition. For neutral particles [$G_{EB}(0) = 0$], we use the same definition with $G_{EB}(0) \to 1$.

In table 8 we present also the decomposition of the octet baryon square radii into valence or bare core (b) and pion cloud (π) contributions. These are defined for $X = E, M$, by

$$(r^2_{XB})_b = -\,Z_B\frac{6}{G_{XB}(0)}\frac{dG_{X0B}}{dQ^2}\bigg|_{Q^2=0}, \tag{6.4}$$

$$(r^2_{XB})_\pi = -Z_B\frac{6}{G_{XB}(0)}\frac{d(\delta G_{XB})}{dQ^2}\bigg|_{Q^2=0}, \tag{6.5}$$

based on the decomposition (3.47). Note that the components $(r^2_{XB})_b$ and $(r^2_{XB})_\pi$ are normalized by the total form factor $G_{XB}(0)$.

In the fitting process we can conclude that the model is very sensitive to the neutron data. This can be a consequence of the impact of the pion cloud in the neutron form factors. [This can also be true for other neutral particles, but there is much more information about the neutron.] A very useful index to study the neutron form factors is the electric square radius. The neutron electric square radius quantifies the slope of the G_{En} form factor at $Q^2 = 0$.

In the present model we can quantify the contribution of the valence quarks and the pion cloud using the decomposition (6.4) and (6.5) for the neutron electric radius ($X = E$). In the present case the result is

$$r^2_{En} = (-0.097)_b + (-0.016)_\pi \ \text{fm}^2. \tag{6.6}$$

From this we conclude that the pion cloud gives about 14% of the total result [-0.113 fm^2, very close to the experimental result -0.116 fm^2]. Again the pion cloud

B	$(r^2_{EB})_b$	$(r^2_{EB})_\pi$	r^2_{EB}	$(r^2_{MB})_b$	$(r^2_{MB})_\pi$	r^2_{MB}
p	0.614	0.168	0.782	0.601	0.117	0.718
n	-0.097	-0.016	-0.113	0.624	0.105	0.729
Λ	-0.005	0.073	0.068	0.449	-0.221	0.228
Σ^+	0.470	0.244	0.713	0.350	0.166	0.516
Σ^0	-0.001	0.040	0.039	0.291	0.097	0.388
Σ^-	0.480	0.162	0.643	0.388	0.253	0.642
Ξ^0	0.096	0.001	0.097	0.325	-0.005	0.319
Ξ^-	0.382	0.021	0.403	0.218	0.050	0.218

Table 8. Octet baryon square radii in vacuum, and the bare and pion cloud contributions.

contribution is still much smaller than suggested by an explicit calculation in the CBM [69]. Nevertheless, this is the best we have been able within the constraints of the fit to the whole octet. We note that the sign of the bare contribution is consistent with the lattice QCD data as we will explain next. Since G_{En} is positive and increases with Q^2 (positive derivative) it gives a negative contribution for r^2_{En}, according to the definition (6.2) [with the replacement $G_{En}(0) \to 1$].

The effects of the valence quarks and pion cloud effects for the octet baryon radii were also estimated in [48]. There, the formalism used is the heavy baryon chiral perturbation theory applied to the lattice QCD data from [49]. In that work of Wang *et al.* [48] the quenched lattice results are corrected by subtracting the quenched and finite volume effects to extract the full QCD result in the physical limit of infinite volume. In this case we estimate the bare contribution from the quenched QCD contribution (QQCD), since in that work it is the component that better approximates the valence quark content. For simplicity we will ignore the uncertainties of the estimates. In that case pion cloud is the dominant contribution (67%) and the slope of the core contribution is positive. The last result suggests that the contribution of the quark core to G_{En} is positive. This is qualitatively consistent with our results, but it is important to quantify the contribution of each term.

In our model the valence quark contribution is determined by the fit to the lattice QCD data and also the nucleon physical data. In both cases the neutron data are included. As discussed in the previous work [27] the spectator quark model simulates the magnitude and sign of the lattice QCD data [88] for G_{En} used in the calibration. That is a consequence of the VMD parametrization where there is an asymmetry between the up (u) and down (d) quarks electromagnetic structure. This is represented by a distinct parametrization of the isoscalar f_{1+} and isovector f_{1-}

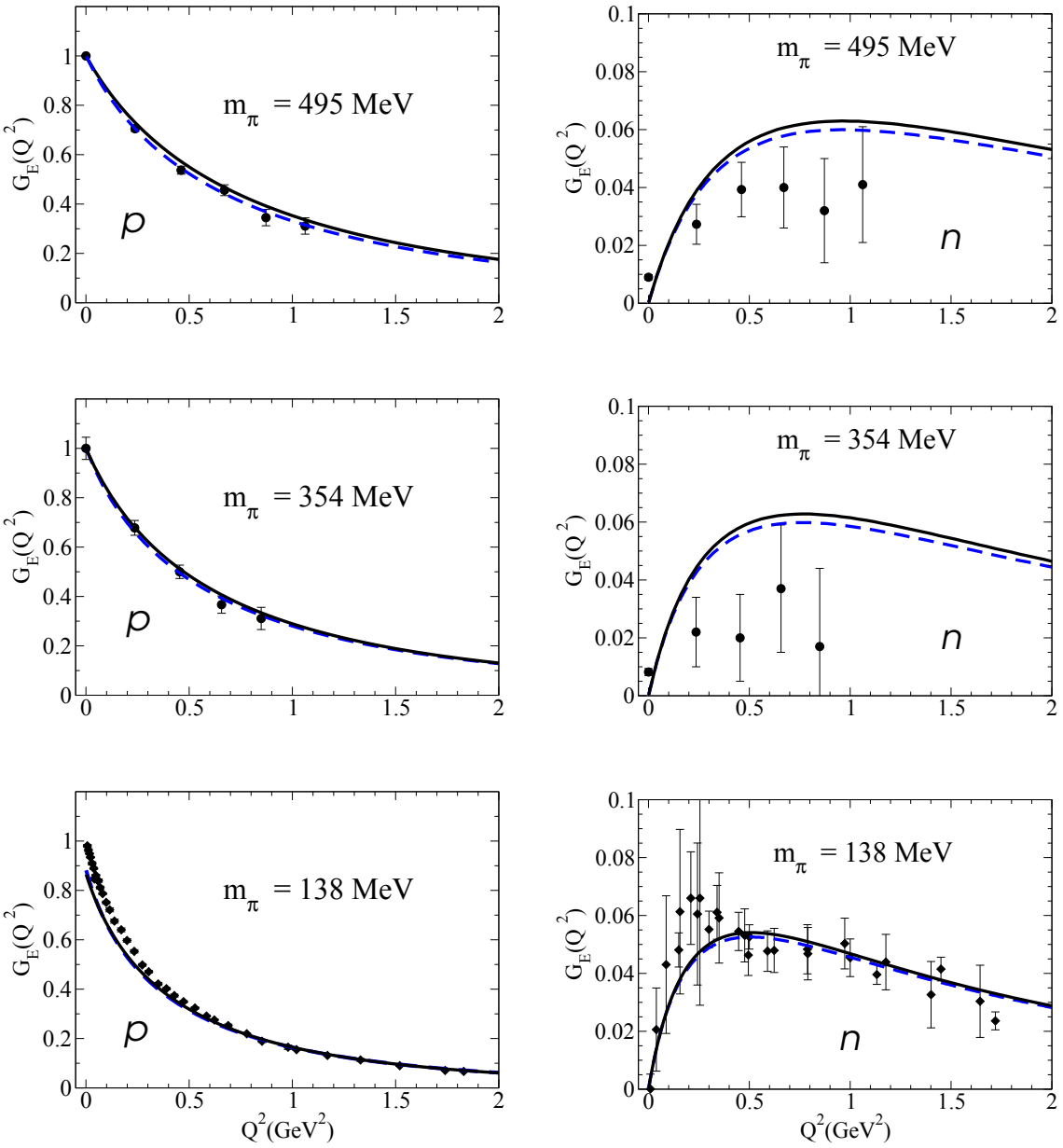

Figure 2. Nucleon electric form factors calculated in lattice, the present model (solid line), and the model from [27] (dashed line). For the physical point $m_\pi = 138$ MeV, only the contributions from the core are included (without the pion cloud).

quark form factors. In particular we have $f_{1+}(Q^2) > f_{1-}(Q^2)$, leading to the result‖ $G_{En}(Q^2) > 0$ for lattice and also for the bare core in the physical case. We note that

‖ Using the expression for the nucleon G_E given by equation (28) of [20], which is equivalent to the

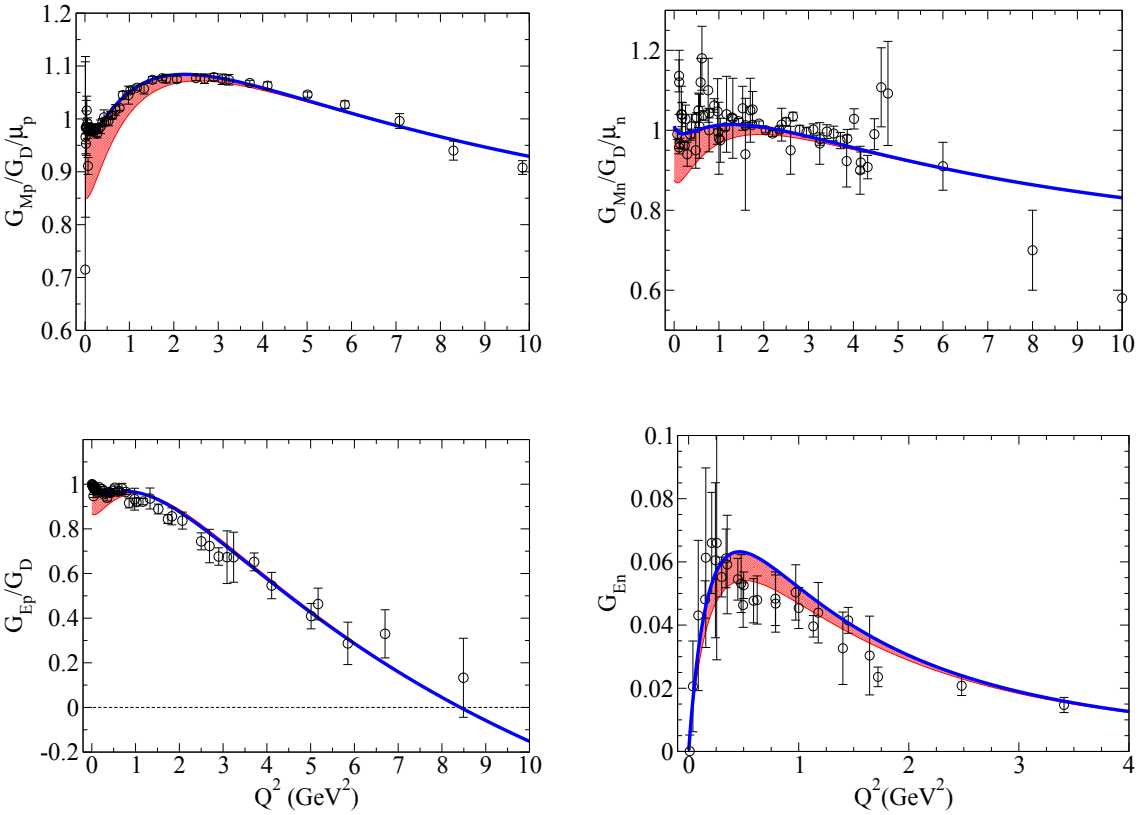

Figure 3. Nucleon form factors fitted at the physical point compared with the experimental data. The bands represent the pion cloud contributions.

although quenched QCD simulations preserve the isospin symmetry, the full QCD simulations and the nature violate (in small degree) the isospin symmetry.

In figure 2 we present the results of the model for the nucleon electric form factors in lattice (G_E), compared with the lattice data from [88] used in the present fit for the cases $m_\pi = 354, 495$ MeV. The calculation is made using the model extended to the lattice regime based on the VMD parametrization [see [27] for more details]. The contributions of the bare core for the physical case ($m_\pi = 138$ MeV) are also presented and compared with the data. In figure 2 we present also the results of the previous model [27], which show that the both models have similar results.

As we can observe from lattice data ($m_\pi = 354$ MeV, and $m_\pi = 495$ MeV) for the neutron, the model results are close to the lattice data, although there are some overestimates of the data. Note also that the neutron lattice data are positive. Since

one used in this work without pion cloud, we have

$$G_{En} = \frac{1}{2} B \left[(f_{1+} - f_{1-}) - \tfrac{Q^2}{4M^2} (f_{2+} - f_{2-}) \right],$$

where B is the overlap integral (normalized to 1 at $Q^2 = 0$). As the Pauli form factors are suppressed in the small Q^2 region, the difference between f_{1+} and f_{1-} determines the sign of G_{En} near $Q^2 = 0$. Taking $G_{Ep} - G_{En}$ we get a dependence in the isovector form factors f_{i-} $(i = 1, 2)$.

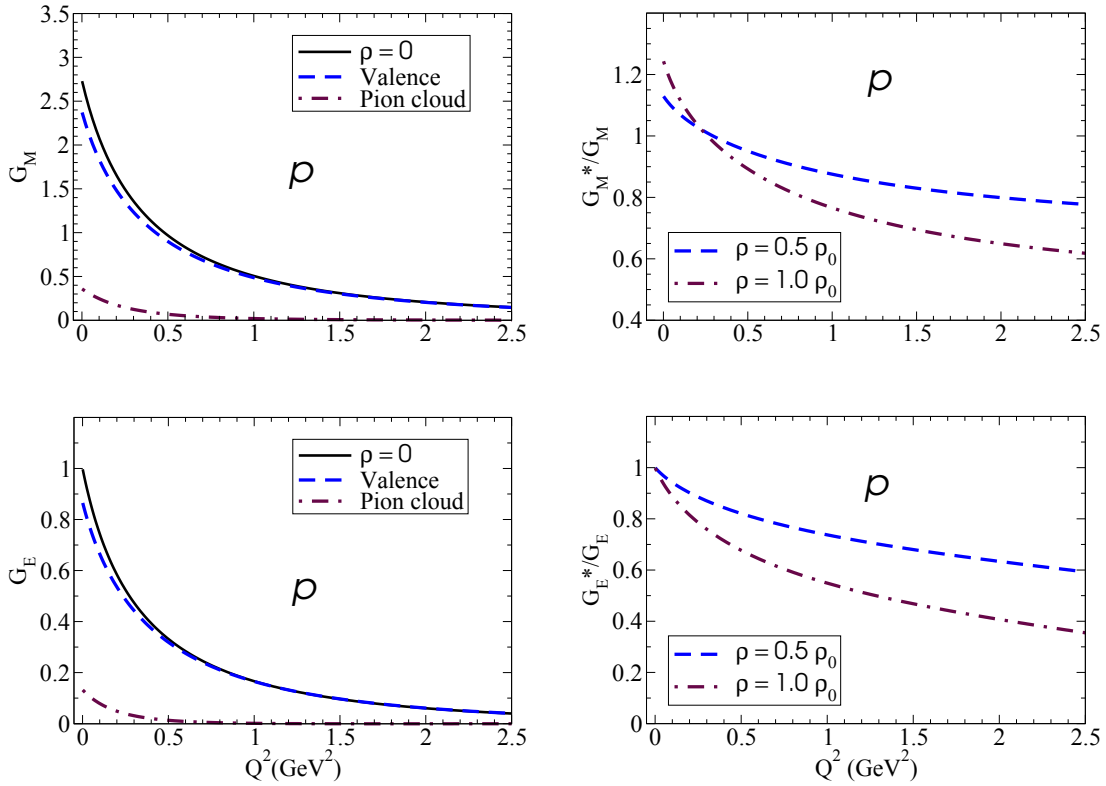

Figure 4. Proton electromagnetic form factors calculated for $\rho = 0$ (vacuum) with a decomposition of the valence and pion cloud contributions (left panel), and the ratios to those of the $\rho = 0$ (right panel) for $\rho = 0.5\,\rho_0$ (dashed line) and $1.0\,\rho_0$ (dash-doted line).

in this lattice QCD regime the pion cloud effects are not important, we interpret the result as a consequence of the isospin asymmetry of the model for the valence quarks as already mentioned. The figure supports our motivation to apply the quark model to the lattice QCD regime, using a model with isospin breaking. One can argue however that since we consider a quark current parameterized by a VMD structure, some pion cloud effects can also be in part of the current, particularly in the term associated with the ρ-pole. [For the high Q^2 region we can claim that the quark structure is the only one that survives consistently with the data.] To analyze better this point we look again for the neutron electric radius. Since the G_{En} data in lattice show a positive increasing function of Q^2 in the low Q^2 region, this implies a negative contribution of the bare core to the charge radius [see equation(6.2)]. The simple comparison of our results with those of Wang *et al.* [48] based on the relative contributions mentioned before (67% of pion cloud in r^2_{En}), can lead a conclusion that about 53% of our VMD parametrization may be pion cloud (67% from Wang's result, and minus 14% in our estimate). Notice, however, that Wang *et al.* uses a different structure for the pion cloud. Contrary to a more common representation for the pion cloud effects in the nucleon system, as the one we adopt (see figure 1) following [90, 91], the work of

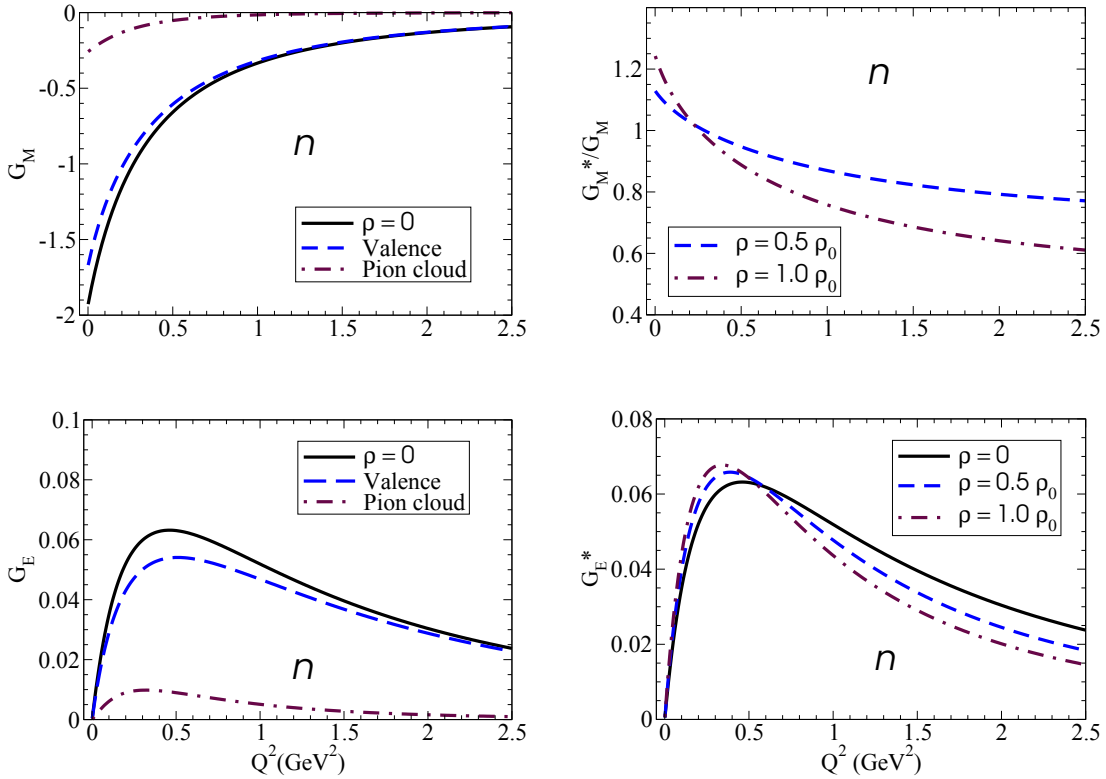

Figure 5. Same as the caption of FIG. 4, but for the neutron. We note that, as discussed in the text, some of the pion cloud contribution in models such as CBM [69, 70] are included through VMD in the valence terms in this parametrization.

Wang *et al.* [48] also includes a diagram with a pion double vertex that comes from full QCD. This diagram can also be a source of the part for the $\sim 50\%$ difference between our estimate and that of [48]. Future studies using lattice QCD simulation data to reduce the model dependence for the pion cloud contributions, combined with a precise estimate for the valence quark structure in the intermediate Q^2 region, can help to pin down the effective contributions of these degrees of freedom.

It can be useful for the nucleon case to compare the lattice QCD data from [88], and our results using the other lattice QCD simulations. There are for instance different data in [92], from the same group, than the data we have used in our calibration. Unfortunately the lattice QCD studies of the nucleon form factors are mainly performed for the nucleon isovector form factors like $G_E^V = G_{Ep} - G_{En}$ and $G_M^V = G_{Mp} - G_{Mn}$, and results for G_{En} have not been published in general. Examples are the works of QCDSF collaboration [93] and the Cyprus group [94, 95]. The main reason to avoid determining the form factors for proton and neutron separately, is because the isoscalar form factors, $G_E^S = G_{Ep} + G_{En}$ and $G_M^S = G_{Mp} + G_{Mn}$, should include contributions from disconnected diagrams [93], which is a complex task with the present lattice QCD resources. The results extracted from [49, 93, 96] are too imprecise to draw any conclusion about the magnitude and the sign of G_{En} on lattice.

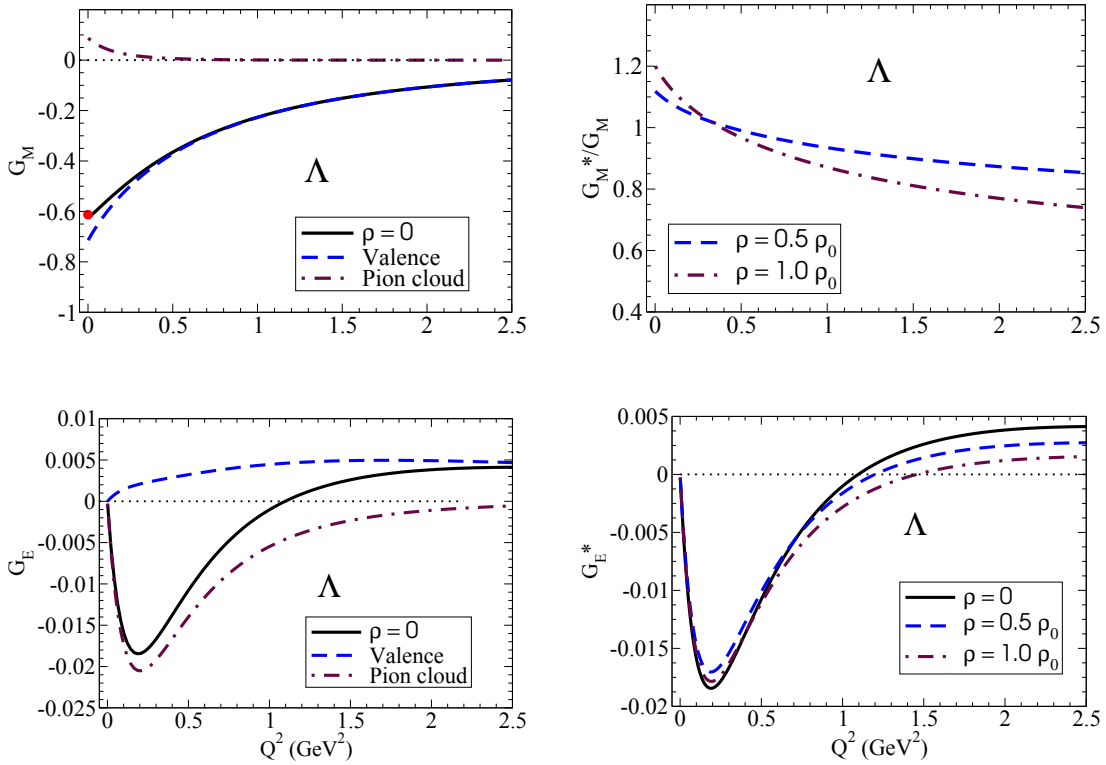

Figure 6. Same as the caption of FIG. 4, but for Λ. The experimental magnetic moment is shown by the (red) dot.

Nucleon isoscalar form factors were calculated recently by the LHPC collaboration [97], and they show also a positive result for G_{En} for pion masses similar to the ones in [88], but larger in magnitude.

Although there are other lattice simulations of the nucleon form factors, we keep our preference for the data in [88], even if the data are affected by some systematic errors as mentioned already [27]. The main reason is the fact that it is the only work extended to the octet baryons. Therefore, the limitations in the neutron form factor results can be compensated by the inclusion of the data for $\Sigma^{+,-}$ and $\Xi^{0,-}$.

The results of the fit for the nucleon form factors are presented in figure 3 and compared with the selected data [74, 75, 76, 77, 78, 79, 80, 81, 82, 83, 84, 85, 86, 87] (see [27] for a detailed discussion about the database). In figure 3 the solid line gives the full result (valence plus pion cloud) and the bands the effect of the pion cloud. The results for the remaining octet baryon members will be presented in the next section and extended to the nuclear medium. Recall that except for the magnetic moments there is no data for the Λ, Σ and Ξ systems. Results in figure 3 show the dominance of the quark core and that the pion cloud effect is restricted to the small Q^2 region. As for the other octet members the form factors are mainly determined by the lattice QCD data. The fit to the lattice data provides a good description (small χ^2 per data point) for the Σ systems but are not so good for the Ξ systems. As for the neutral particles, Λ, Σ^0 and Ξ^0, our calibration provide only a crude estimate of

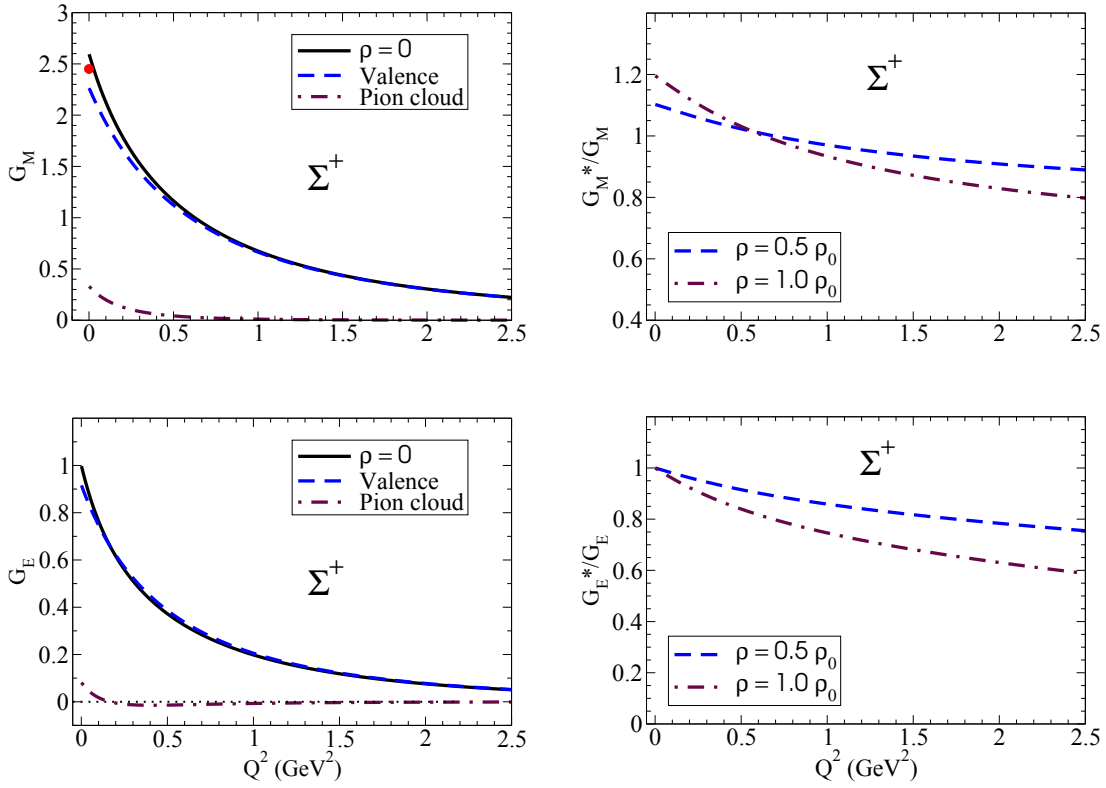

Figure 7. Same as the caption of FIG. 4, but for Σ^+. The experimental magnetic moment is shown by the (red) dot.

the core effect, since these systems are not constrained by lattice data (except for Ξ^0). Therefore, the separation between the core and pion cloud should be taken with care particularly for G_E (very small for neutral particles), where small pion cloud effects and residual quark core effects cannot be distinguished with precision.

Other properties of the octet baryons in vacuum are listed in Tables 7 and 8. From Table 7 we can conclude that the present model can describe fairly well the octet square radii and the magnetic moments, except for Ξ^0. From Table 8 we note the dominance of the quark core effects on the octet baryon radii. The exception is the electric square radii of the charge neutral particles, as mentioned already. A note about the large pion cloud contribution for the Σ^- magnetic square radii, is in order. The large pion cloud contribution for $r^2_{M\Sigma^-}$ is essentially a consequence of the large contribution of the term in $\tilde{B}_2$ (photon-pion coupling contribution for F_{2B}). In fact the same effect appears for Σ^+, but the final value is reduced by the larger magnetic moment (factor 2.28), in the definition of r^2_{MB} [see equation (6.3)].

Before extending the model for the in-medium regime, we discuss the sensitivity of the model to the input data. As already mentioned, we restrict the range of variation of $r^2_{E\Sigma^-}$ to 0.610 ± 0.015 fm^2, instead of using the experimental result 0.61 ± 0.15 fm^2 [67]. The main effect of this constraint is the reduction of the pion cloud contribution for $r^2_{E\Sigma^-}$ to a value ≈ 0.2 fm^2, similar to that for the proton. Also the contribution for the

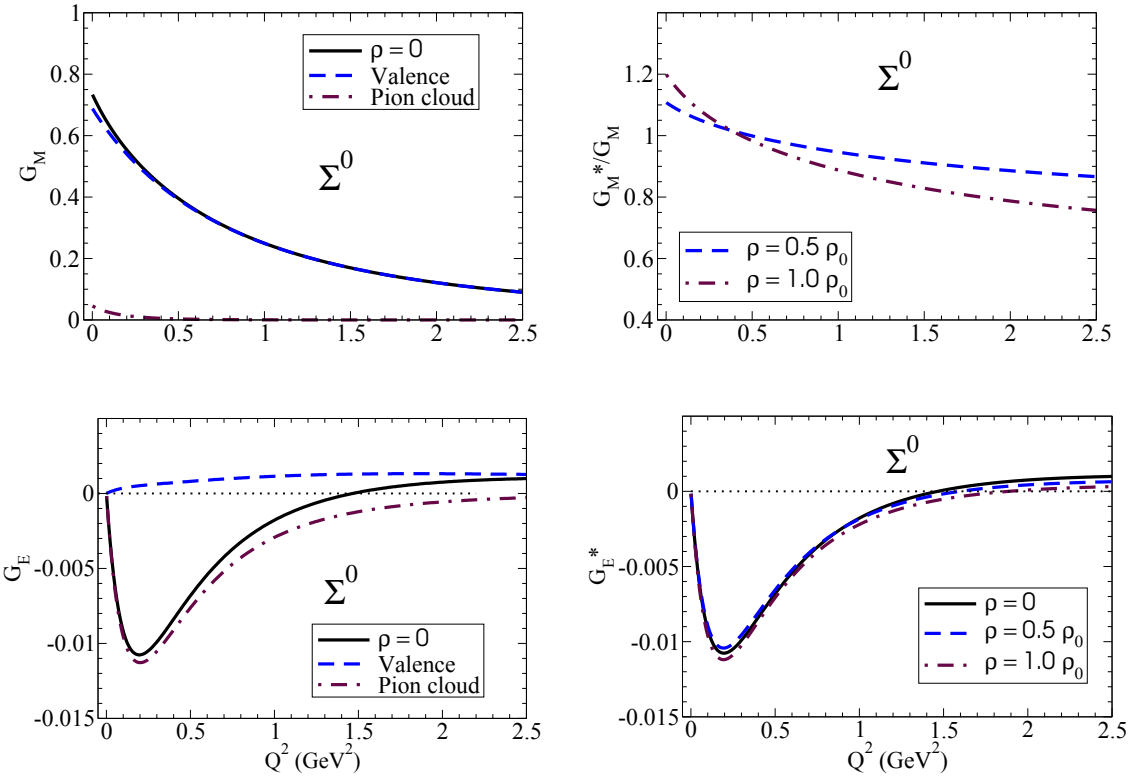

Figure 8. Same as the caption of FIG. 4, but for Σ^0.

Σ^+ electric square radius, (less than twice the value for Σ^-) is similar in magnitude. We can then conclude that the parameters of the model are very sensitive to the values of $r^2_{E\Sigma^-}$ and $r^2_{E\Sigma^+}$, and the respective contributions of the pion cloud. Thus, precise measurements of $r^2_{E\Sigma^-}$ and $r^2_{E\Sigma^+}$ should be very useful to improve the quality of the model, and also to check if the assumption $r^2_{E\Sigma^-} \approx r^2_{Ep}$, is justified or not.

A few notes about the quality of the results for the octet baryon results are in order. The quality of the fit is better for the systems with a strange quark, Λ, Σ, than the ones with two strange quarks, Ξ. We recall that the kaon cloud contribution neglected for the Ξ-baryon in the present approach, may be important since the contribution of the pion cloud is small. Therefore the prediction for Σ are expected to be more reliable than that for Ξ. Also, as no lattice data for Λ and Σ^0 are used in the calibration of the model, the results for the charge neutral particles, Λ, Σ^0, Ξ^0, have to be taken with caution, particularly for the separation of valence and pion cloud contributions as discussed about the radii. Nevertheless, we present the results for the all charge neutral particles for completeness. Finally, we note that the predictions for the high Q^2 region has also to be taken with care, since the lattice data used in the calibration are restricted to $Q^2 < 1.5$ GeV^2. The nucleon case is an exception (see figure 3), since (physical) data are available for high Q^2.

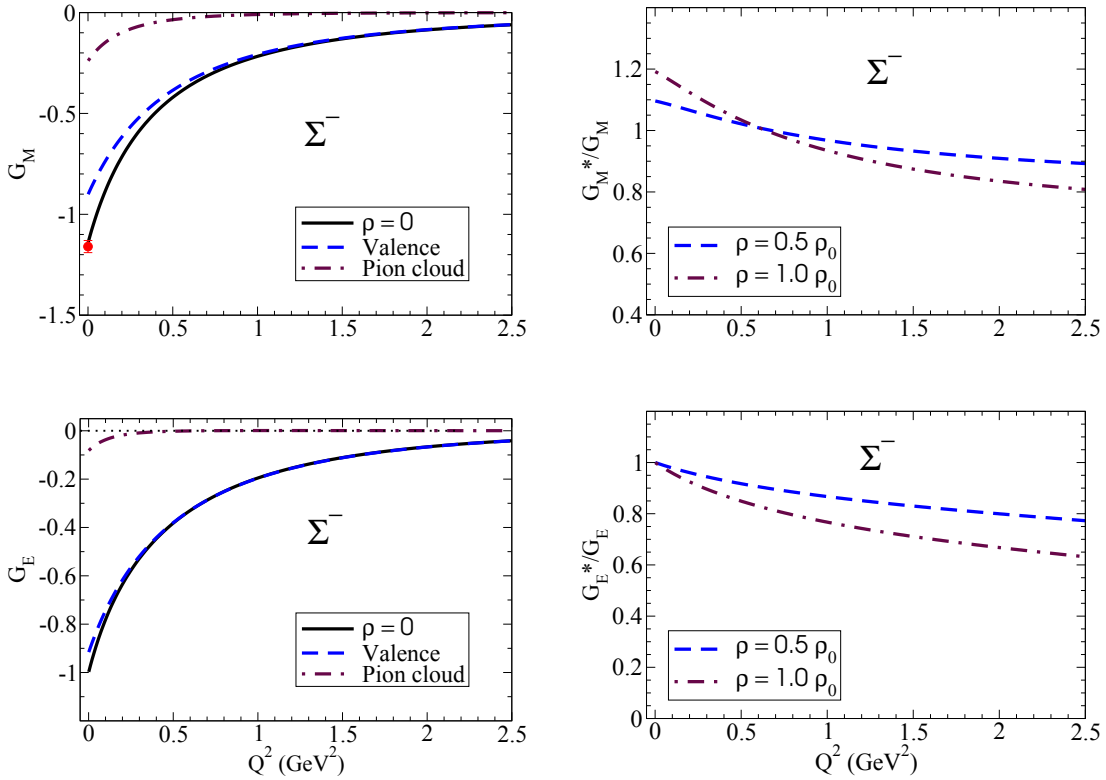

Figure 9. Same as the caption of FIG. 4, but for Σ^-. The experimental magnetic moment is shown by the (red) dot.

6.2. Octet baryon electromagnetic form factors in medium

We consider now the octet baryon electromagnetic form factors in the nuclear medium. The formalism and the parameters necessary have already been presented in section 5. We calculate G_E^* and G_M^* for nuclear matter densities $\rho = 0.5\,\rho_0$ and $\rho = \rho_0$ with $\rho = 0.15$ fm^{-3}. The modification of the form factors in the nuclear medium may be characterized by the in-medium modified masses given in Table 3, and the modified coefficients β_B^* given in Table 4.

The results are presented in figures 4-11. On the left panel in each figure the results in vacuum ($\rho = 0$) are presented, where also the valence quark contribution (dashed line) and the pion cloud contribution (dash-dot line) are shown. On the right panel, in-medium to vacuum ratios of the form factors are shown. For the charge neutral particles $(n, \Lambda, \Sigma^0, \Xi^0)$, instead, the absolute values of $G_E^*(Q^2)$ are shown, since $G_E(0) = G_E^*(0) = 0$ and because the values are in general small for finite Q^2 compared to $G_M^*(Q^2)$. For these cases the vacuum values are presented with the thick-solid lines. The experimental magnetic moments in vacuum [67] are also shown for the cases $B = \Lambda, \Sigma^{+,-}, \Xi^{0,-}$ with the filled circles.

From the figures it is clear that generally the valence quark contributions are more than 80% of the total contribution of each octet baryon form factor, and this is in agreement with the results of [27]. The exceptions are the electric form factors

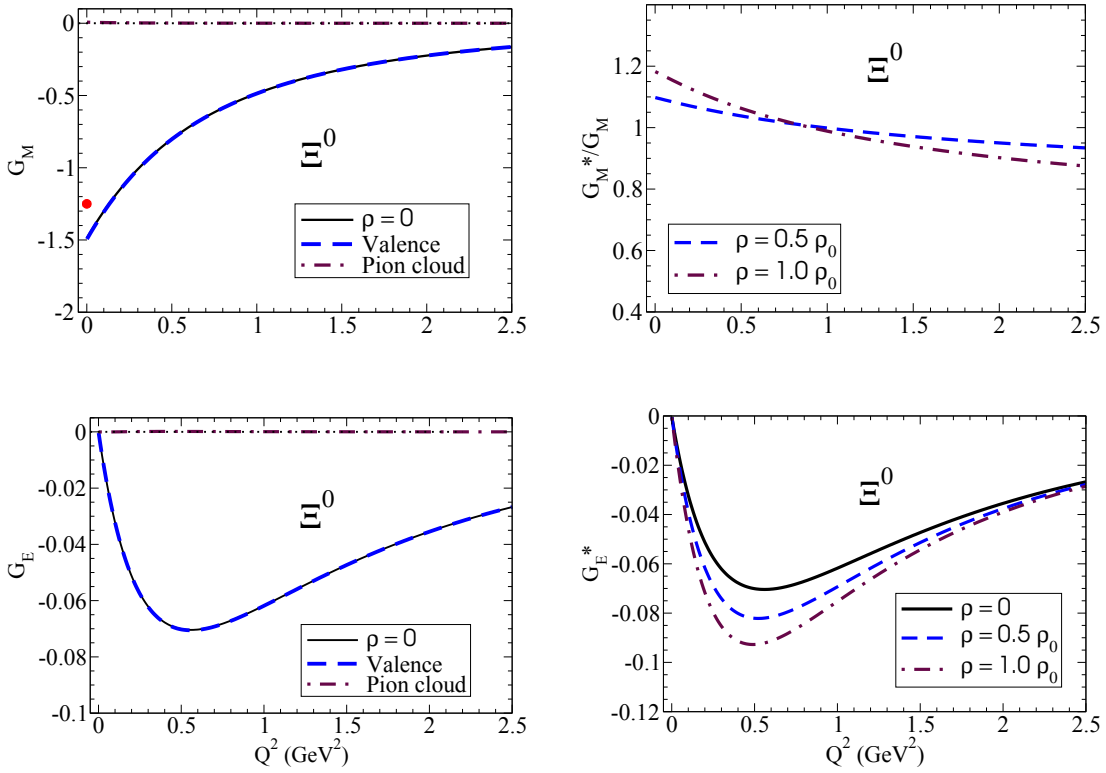

Figure 10. Same as the caption of FIG. 4, but for Ξ^0. The experimental magnetic moment is shown by the (red) dot.

of the charge neutral particles n, Λ, Σ^0 and Ξ^0. To estimate the pion cloud effects in the nuclear medium, we note that the ratio of the pion coupling constant in-medium to vacuum, $g^*_{\pi BB'}/g_{\pi BB'}$, given in Table 4 is at most 10%. As the factors β_B depend quadratically from the ratio $g^*_{\pi BB'}/g_{\pi BB'}$, the effect of the variation in medium can be up to 20%. Since the largest case of the pion cloud contribution in vacuum electromagnetic form factors is about 20% (aside from the electric form factors of the neutral baryons), the total modification in medium associated with the pion cloud is at most 4% (20% of 20%). Thus, the pion cloud effects in the nuclear medium are essentially the same as those in vacuum, which are shown in the left panels in figures 4-11. Thus, the significant modification of the form factors in medium which is shown in the right panels in figures 4-11, is according to the in-medium modification of the valence quark contributions, which are much more sensitive to the in-medium modification than those of the pion cloud. The strong sensitivity of the valence quark contributions is a consequence of the medium modification of the vector meson masses (modification of the VMD based quark current) and the baryon masses, which are in the radial wavefunctions.

However, the smallness of in-medium change of the pion cloud contributions for the electromagnetic form factors (at most 4%), does not apply for the electric form factors of n, Λ, Σ^0 and Ξ^0, since a priori these electric form factors are very small

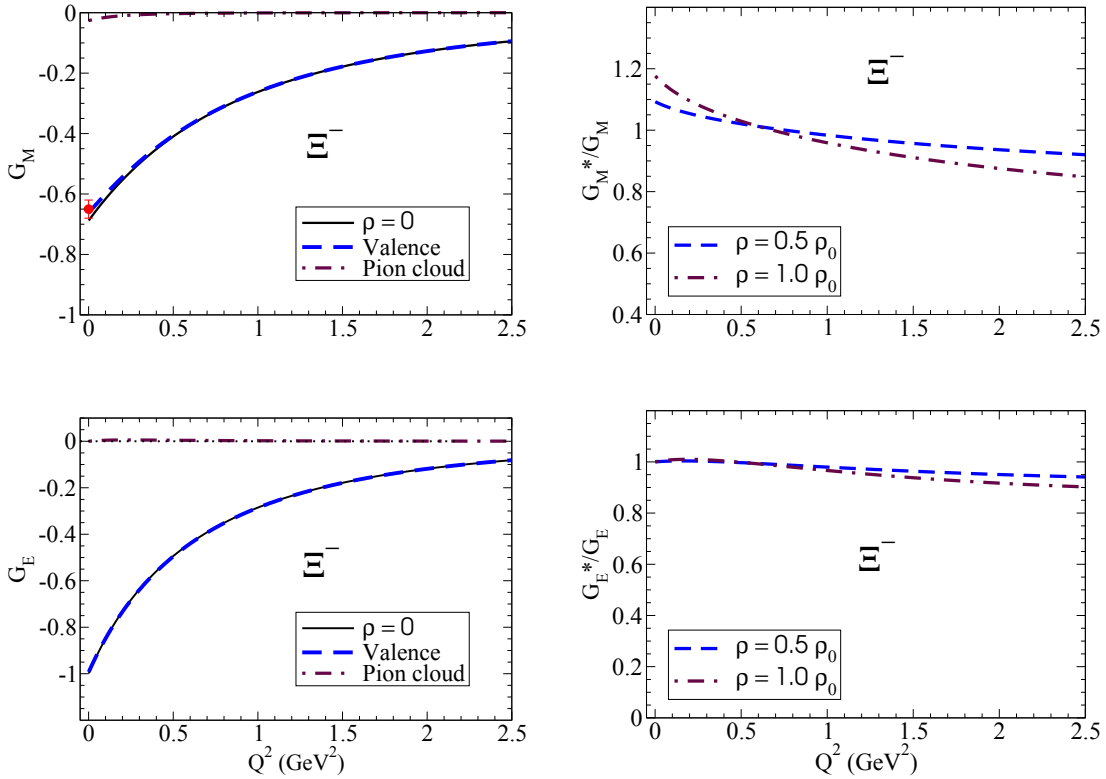

Figure 11. Same as the caption of FIG. 4, but for Ξ^0. The experimental magnetic moment is shown by the (red) dot.

$G_E^* \approx Q^2$ near $Q^2 = 0$. In these cases it would be much informative to look the direct contribution of the pion cloud contribution in medium, not the ratio, since it can be dominant. In this way, we show the pion cloud contributions in vacuum and in medium in figure 12. By comparing the scales we can conclude that the pion cloud contributions are small for the neutron and Ξ^0, but they are the leading contributions for Λ and Σ^0. For the neutron the contributions are about 0.01, to be compared with the total magnitude 0.06 (see figure 5). As for the Ξ^0, the pion cloud contributions are negligible (compare the scales of G_E^* in figure 10 and figure 12), which is a consequence of the small coupling constant ($\beta_\Xi \approx 0.04$). Finally for Λ and Σ^0, as shown in figures 6 and 8, the pion cloud gives dominant contributions in the region $Q^2 < 1$ GeV^2, although the valence quarks become dominant for higher Q^2. Thus, we conclude that, although the pion cloud gives dominant contributions for Λ and Σ^0, the medium modification of the form factors according to the pion cloud is small.

We look now for the global result in medium. For the electric form factors we notice that the ratio G_E^*/G_E decreases from unity for increasing Q^2 (except the discussions for the charge neutral particles), which means that the electric form factors in medium decrease faster than those in vacuum. The medium effect is very small for Ξ^- (ratio is almost constant) reflecting the lower sensitivity of the strange quark to the medium modifications). As for the magnetic form factors they are enhanced by

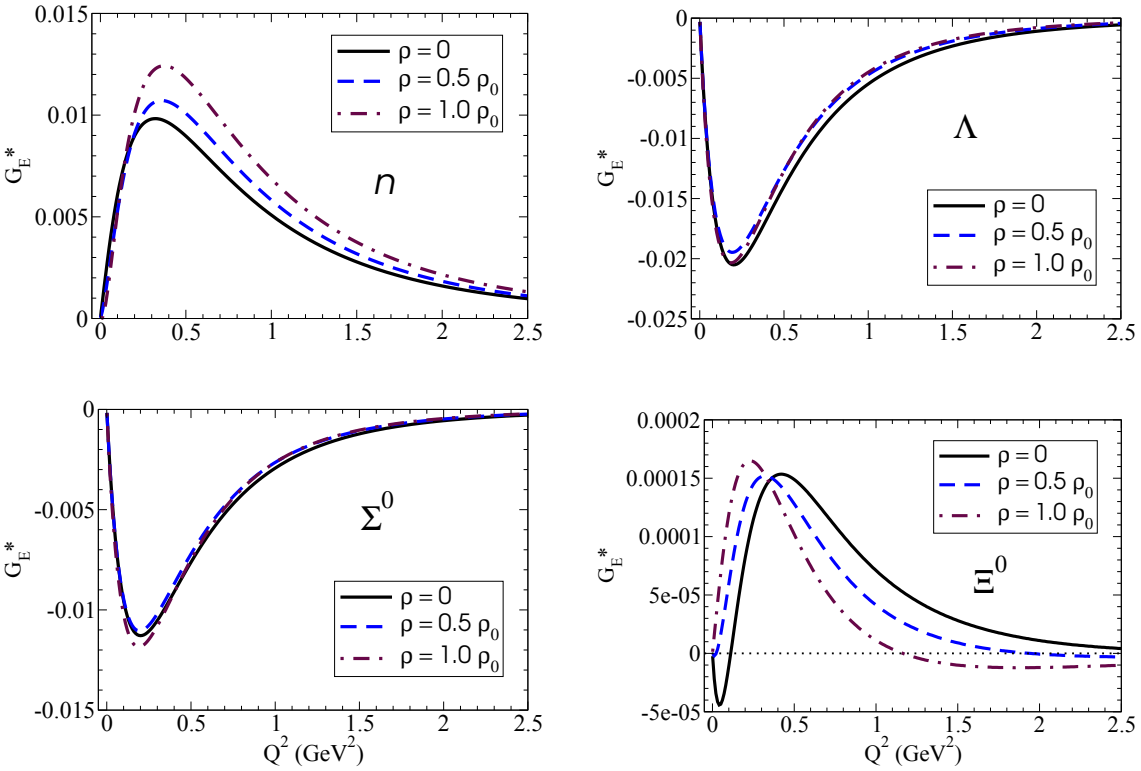

Figure 12. Pion cloud contributions for G_E^* in nuclear matter for charge neutral particles.

the medium for small Q^2. The effect is larger for larger densities. In [10] proton electromagnetic form factors in medium were studied. The results presented in [10] show similar trends to those observed in the present study. Namely, the in-medium magnetic form factor is enhanced, while that of the electric form factor is quenched, where these results can explain the modification of the bound proton form factors measured at Jefferson Lab [5]. The modifications of the nucleon electromagnetic form factors in medium will be discussed in next subsection.

In the literature we find only [98] studied medium modification of the octet baryon magnetic moments aside from the nucleon, using a different kind of quark-meson coupling model from the present one, "QMC" and modified quark-meson coupling model (MQMC). In their treatment, the pion or meson cloud is not included in the electromagnetic currents. (We discuss the nucleon case in next section.) They compared with "QMC" and MQMC results for the magnetic moments in nuclear medium. In their "QMC", the in-medium magnetic moments for the Λ and Ξ^- decrease compared to those in vacuum, although other octet magnetic moments are all increased in medium. This feature is different from the present approach, where all the octet baryon magnetic moments ($G_M^*(Q^2)$ at $Q^2 = 0$) are enhanced in medium. In their MQMC, on the other hand, all the octet magnetic moments are enhanced, and this feature is the same as that of the present approach.

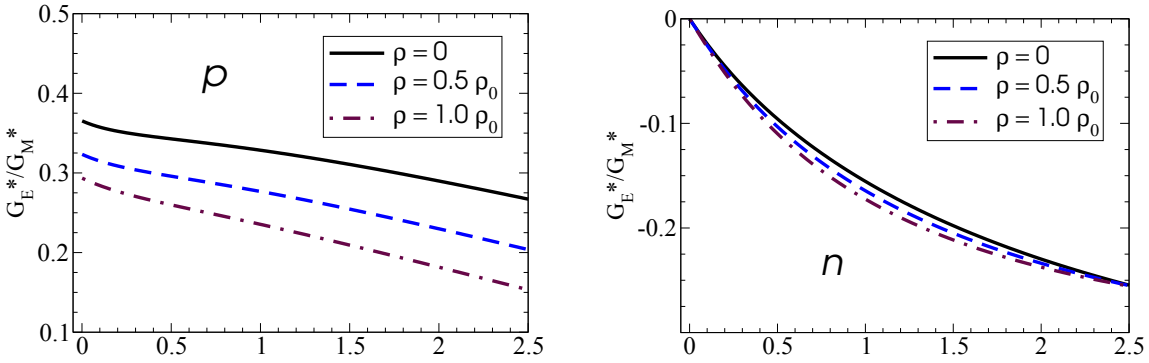

Figure 13. Ratios G_E^*/G_M^* in nuclear matter for the proton (left) and neutron (right).

6.2.1. Nucleon electromagnetic form factors in-medium. We study now in detail the medium modification of the nucleon electromagnetic form factors. A very interesting quantity is the ratio of the electric to the magnetic form factors,

$$R_N^* = \frac{G_{EN}^*}{G_{MN}^*}, \tag{6.7}$$

which can be also calculated in vacuum (denoted by R_N). The study of this ratio for the proton in vacuum serves as a fundamental quantity in the present understanding of the proton structure, as was measured at Jefferson Lab, that R_p significantly deviates from a constant [74, 75]. Similar studies were also made for the neutron [81, 82, 99].

In figure 13 we present our predictions for the both, proton and neutron ratios in medium, for nuclear densities $\rho = 0.5\,\rho_0$ and $\rho = 1.0\,\rho_0$. Note that $\rho = 0$ (vacuum) case was already compared with the experimental data in the present model since it fits both G_E and G_M (see figure 2). Experimentally, direct access for the ratio R_N^* in-medium seems to be impossible at present. However, we can get indirect information for the in-medium ratios using the results of proton (nucleon) recoil polarization experiments in nuclei by the measurement of the polarization-transfer super-ratio for the nucleon,

$$\mathcal{R} = \frac{G_E^*/G_M^*}{G_E/G_M}. \tag{6.8}$$

The experiments were performed for the proton using ^{1}H, ^{4}He, and ^{16}O targets [4, 5, 6], and also planed for the neutron case [8, 9].

The results of our predictions for $\mathcal{R}$ for the proton and the neutron are presented in figure 14. Some other calculations for the proton case can be found in [10, 11, 13, 100, 101, 102, 103, 104], and summarized in [2, 9]. For a detailed discussions about the super-ratio of the proton and the neutron, see [2, 8, 105].

First, we discuss the proton super-ratio shown in the left panel in figure 14 with the data with the ^{4}He target from [4, 5, 6]. Our results for $\rho = 0.5\,\rho_0$ ($\rho_0 = 0.15$ fm^{-3}) reproduce the data. While the average nuclear density of ^{4}He is expected to be slightly higher ($0.74\,\rho_0$ in a QMC estimate) the effect of absorption means that the active nucleon tents to be in the nuclear surface. Thus, the present model predicts the observed trend of the reduction for the super-ratio.

Next, turning the discussion to the neutron case, our results predict an *enhancement* of the super-ratio, contrary to the case of the proton. The enhancement was also predicted by Nambu-Jona-Lasinio (NJL) model and relativistic light front constituent quark model (LFCQ) [8]. However, the difference is the Q^2 dependence. In the case of the NJL model, the super-ratio monotonically decreases with increasing Q^2, while it stays almost constant in LFCQ. The present result shows appreciable Q^2 dependence, namely the ratio increases up to around $Q^2 = 0.3$ GeV^2, and gradually decreases with increasing Q^2. Thus, our model predicts that the modification can be maximally observed around $Q^2 = 0.3$ GeV^2. This point may be taken into consideration in the experiments planned [9].

7. Summary and conclusions

In this work we have presented a model for the octet baryon electromagnetic form factors in vacuum and in the nuclear medium. The model is based on a constituent quark formalism but includes also a phenomenological parametrization for the pion cloud motivated by χPT. The octet baryon and relevant meson properties in the nuclear medium (masses and coupling constants) are determined using the QMC model. The effects of final state interactions and meson exchange current are not explicitly included.

The model is calibrated by the octet baryon lattice data (electromagnetic form factors), as well as physical data, such as the nucleon electromagnetic form factors, octet baryon magnetic moments and the available octet baryon radii data. Lattice data give stringent constraints for the valence quark structure of the octet baryons. The remaining data combined with the estimate of the valence quark core contributions, constrain the parametrization of the pion cloud.

The fit is very sensitive to the neutron lattice data for the electric form factor and also to the value of the Σ^- electric radius. The neutron data, lattice and physical, are well described by a valence quark model with isospin breaking. An accurate description of the data, including the octet radii (nucleon and Σ^-) is also obtained with a small value for electric square radii for Σ^- (≈ 0.6 fm^2) which is a consequence of a small pion cloud contribution for the electric radius (same order as that for the proton).

Future improvements are possible. Accurate lattice data, particularly for the neutron electric form factor (G_{En}) can clarify the role of the valence quark contributions, and eventually demand a refit of the quark current used in this work. The available lattice data support a quark electromagnetic current with an isospin breaking, but new data with a smaller effect for G_{En} may require a model with almost no isospin breaking. The model can also be improved by including a pion cloud parametrization derived from first principle QCD, utilizing the results of lattice simulations (see Ref. [48]).

The explicit inclusion of meson exchange current corrections in the electromagnetic form factors in a consistent manner, may be appreciable at high momentum transfer, especially if the absolute values of form factors became very small, or for the electric form factors of neutral baryons.

We predict that all the octet baryon magnetic form factors in medium will be enhanced in the small Q^2 region, and the magnetic moments of the octet baryons in medium are enhanced. The model predicts that Q^2 dependence of the octet baryon electric form factors in medium decreases faster than those in vacuum. Furthermore,

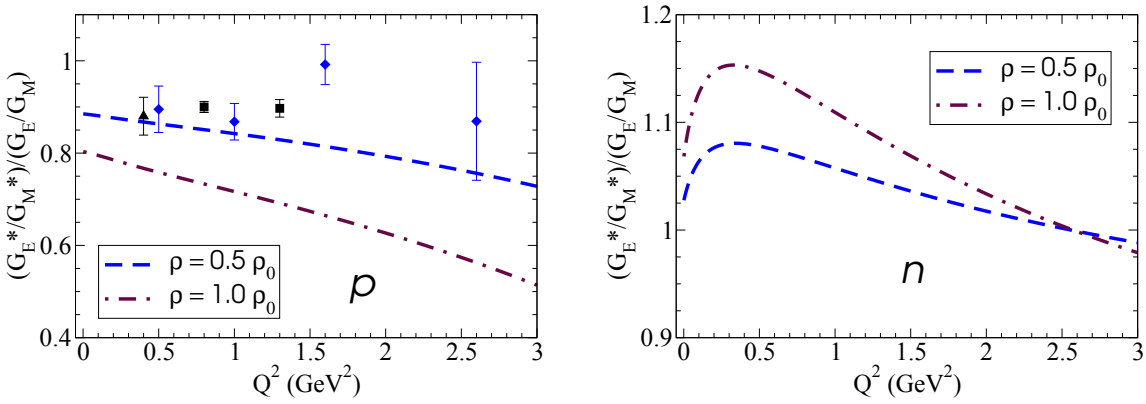

Figure 14. Super-ratios in nuclear matter calculated for the proton (left) and neutron (right). Data for proton are from [4, 5, 6].

the present model predicts also a decrease of the super-ratio for the proton in the nuclear medium, which is in agreement with the observed results. On the other hand, for the neutron super-ratio in the nuclear medium, the present model predicts the *enhancement*, which has its maximum around $Q^2 = 0.3$ GeV^2, and this may be useful information for the planned experiments.

Acknowledgments:

We thank K. Saito for useful discussions and warm hospitality (K.T.) at Tokyo University of Science, Noda, Japan, where part of the work was undertaken. G.R. would like to acknowledge CSSM at the University of the Adelaide for making it possible for him to visit and stay. This work was supported in part by the European Union (HadronPhysics2 project "Study of strongly interacting matter"), by the University of Adelaide and by the Australian Research Council through grant No. FL0992247 (AWT). G.R. was supported by the Fundação para a Ciência e a Tecnologia under the Grant No. SFRH/BPD/26886/2006. K.T. would like to acknowledge the International Institute of Physics, Federal University of Rio Grande do Norte, Natal, Brazil, for a visiting professorship during which part of this work was carried out.

References

[1] Brown G E and Rho M 1991 Phys. Rev. Lett. **66** 2720
[2] For a recent experimental review: Brooks W K, Strauch S and Tsushima K 2011 J. Phys. Conf. Ser. **299** 012011
[3] Malov S, Wijesooriya K, Baker F T, Bimbot L, Brash E J, Chang C C, Finn F M, Fissum K G *et al.* 2000 Phys. Rev. **C62** 057302
[4] Dieterich S, Bartsch P, Baumann D, Bermuth J, Bohinc K, Bohm R, Bosnar D, Derber S *et al.* 2001 Phys. Lett. **B500** 47
[5] Strauch S *et al.* [Jefferson Lab E93-049 Collaboration] 2003 Phys. Rev. Lett. **91** 052301
[6] Paolone M, Malace S P, Strauch S, Albayrak I, Arrington J, Berman B L, Brash E J, Briscoe B *et al.* 2010 Phys. Rev. Lett. **105** 072001
[7] Malace S P, Paolone M, Strauch S, Albayrak I, Arrington J, Berman B L, Brash E J, Briscoe B *et al.* 2011 Phys. Rev. Lett. **106** 052501
[8] Cloet I C, Miller G A, Piasetzky E and Ron G 2009 Phys. Rev. Lett. **103**, 082301

[9] Ron G *et al.* Jefferson Lab PAC35 Letter of Intent, 14 December, 2009, http://hallaweb.jlab.org/collab/PAC/PAC35/LOI-10-007-Neutron-Modification.pdf
[10] Lu D H, Thomas A W, Tsushima K, Williams A G and Saito K 1998 Phys. Lett. B **417** 217
Lu D H, Tsushima K, Thomas A W, Williams A G and Saito K 1998 Phys. Lett. B **441** 27
Lu D H, Tsushima K, Thomas A W, Williams A G and Saito K 1999 Phys. Rev. C **60** 068201
[11] Smith J R and Miller G A 2004 Phys. Rev. C **70** 065205
[12] Horikawa T and Bentz W 2005 Nucl. Phys. A **762** 102
[13] Schiavilla R, Benhar O, Kievsky A, Marcucci L E and Viviani M 2005 Phys. Rev. Lett. **94** 072303
[14] Tsushima K, Riska D O and Blunden P G 1993 Nucl. Phys. A **559** 543
[15] Tsushima K, Kim H C and Saito K 2004 Phys. Rev. C **70** 038501
[16] Gari M and Hyuga M 1976 Nucl. Phys. A **264** 409
[17] Maize M A and Kim Y E 1983 Nucl. Phys. A **407** 507
[18] Hadjimichael E, Goulard B and Bornais R 1983 Phys. Rev. C **27** 831
[19] Schiavilla R and Riska D O 1991 Phys. Rev. C **43** 437
[20] Gross F, Ramalho G and Peña M T 2008 Phys. Rev. C **77** 015202
[21] Gross F, Ramalho G and Peña M T 2012 Phys. Rev. D **85** 093005
[22] Gross F, Ramalho G and Peña M T 2012 Phys. Rev. D **85** 093006
[23] Gross F, Ramalho G and Peña M T 2008 Phys. Rev. C **77** 035203
[24] Ramalho G, Peña M T and Gross F 2008 Eur. Phys. J. A **36** 329
[25] Gross F 1969 Phys. Rev. **186** 1448
Gross F, Van Orden J W and Holinde K 1992 Phys. Rev. C **45** 2094
[26] Gross F, Ramalho G and Tsushima K 2010 Phys. Lett. B **690** 183
[27] Ramalho G and Tsushima K 2010 Phys. Rev. D **84** 054014
[28] Ramalho G and Peña M T 2009 J. Phys. G **36** 085004
[29] Ramalho G, Peña M T and Gross F 2009 Phys. Lett. B **678** 355
[30] Ramalho G, Peña M T and Gross F 2010 Phys. Rev. D **81** 113011
[31] Ramalho G, Tsushima K and Gross F 2009 Phys. Rev. D **80** 033004
[32] Ramalho G and Peña M T 2011 Phys. Rev. D **83** 054011
[33] Ramalho G, Peña M T and Gross F 2008 Phys. Rev. D **78** 114017
[34] Ramalho G and Peña M T 2009 Phys. Rev. D **80** 013008
[35] Ramalho G and Peña M T 2009 J. Phys. G **36** 115011
[36] Ramalho G and Peña M T 2012 Phys. Rev. D **85** 113014
[37] Ramalho G and Tsushima K 2010 Phys. Rev. D **81** 074020
[38] Ramalho G and Peña M T 2011 Phys. Rev. D **84** 033007
Ramalho G and Tsushima K 2011 Phys. Rev. D **84** 051301
Ramalho G, Jido D and Tsushima K 2012 Phys. Rev. D **85** 093014
[39] Guichon P A M 1988 Phys. Lett. **B200** 235
[40] Saito K, Tsushima K and Thomas A W 2007 Prog. Part. Nucl. Phys. **58** 1
[41] Guichon P A M, Saito K, Rodionov E N and Thomas A W 1996 Nucl. Phys. A **601** 349
Saito K, Tsushima K and Thomas A W 1996 Nucl. Phys. A **609** 339
[42] Saito K, Tsushima K and Thomas A W 1997 Phys. Rev. C **55** 2637
[43] Tsushima K, Saito K, Haidenbauer J and Thomas A W 1998 Nucl. Phys. A **630** 691
[44] Guichon P A M, Thomas A W and Tsushima K 2008 Nucl. Phys. A **814** 66
[45] Tsushima K and Khanna F C 2004 J. Phys. G **30** 1765
Tsushima K and Khanna F C 2003 Prog. Theor. Phys. Suppl. **149** 160
Tsushima K and Khanna F C 2003 Phys. Rev. C **67** 015211
[46] Shyam R, Tsushima K and Thomas A W 2009 Phys. Lett. B **676** 51
Shyam R, Tsushima K and Thomas A W 2012 Nucl. Phys. A **881** 255
[47] Tsushima K, Saito K, Thomas A W and Wright S V 1998 Phys. Lett. B **429**, 239 [Erratum-ibid. B **436** 453]
Tsushima K, Lu D H, Thomas A W and Saito K 1998 Phys. Lett. B **443** 26
Tsushima, Lu D H, Thomas A W, Saito K and Landau R H 1999 Phys. Rev. C **59** 2824
Sibirtsev A, Tsushima K, Saito K and Thomas A W 2000 Phys. Lett. B **484** 23
Tsushima K and Khanna F C 2003 Phys. Lett. B **552** 138
Krein G, Thomas A W and Tsushima K 2011 Phys. Lett. B **697** 136
Tsushima K, Lu D H, Krein G and Thomas A W 2011 Phys. Rev. C **83** 065208
[48] Wang P, Leinweber D B, Thomas A W and Young R D 2009 Phys. Rev. D **79** 094001
[49] Boinepalli S, Leinweber D B, Williams A G, Zanotti J M and Zhang J B 2006 Phys. Rev. D **74** 093005
[50] Kubodera K, Kohyama Y, Oikawa K and Kim C W 1985 Nucl. Phys. A **439** 695

[51] Leinweber D B, Boinepalli S, Cloet I C, Thomas A W, Williams A G, Young R D, Zanotti J M and Zhang J B 2005 Phys. Rev. Lett. **94** 212001
[52] Franklin J 2002 Phys. Rev. D **66** 033010
[53] Kubis B, Hemmert T R and Meissner U G 1999 Phys. Lett. B **456** 240
[54] Cheedket S, Lyubovitskij V E, Gutsche T , Faessler A, Pumsa-ard K and Yan Y 2004 Eur. Phys. J. A **20** 317
[55] Jenkins E E, Luke M E, Manohar A V and Savage M J 1993 Phys. Lett. B **302** 482
[56] Meissner U G and Steininger S 1997 Nucl. Phys. B **499** 349
[57] Puglia S J and Ramsey-Musolf M J 2000 Phys. Rev. D **62** 034010
[58] Geng L S, Martin Camalich J, Alvarez-Ruso L and Vicente Vacas M J 2008 Phys. Rev. Lett. **101** 222002
[59] Gell-Mann M 1962 Phys. Rev. **125** 1067
[60] Carruthers P 1966 *Introduction to Unitary Symmetry*, (John Wiley and Sons, Inc. New York), p. 118
[61] Leinweber D B, Lu B H and Thomas A W 1999 Phys. Rev. D **60** 034014
[62] Young R D, Leinweber D B and Thomas A W 2005 Phys. Rev. D **71** 014001
[63] Hall J M M, Leinweber D B and Young R D 2012 Phys. Rev. D **85** 094502
[64] Hammer H W, Drechsel D and Meissner U G 2004 Phys. Lett. B **586** 291
[65] Bernard V, Kaiser N and Meissner U G 1995 Int. J. Mod. Phys. E **4** 193
[66] Perdrisat C F, Punjabi V and Vanderhaeghen M 2007 Prog. Part. Nucl. Phys. **59** 694
[67] Nakamura K *et al.* [Particle Data Group] 2010 J. Phys. G **37** 075021
[68] Brodsky S J and Farrar G R 1975 Phys. Rev. D **11** 1309
[69] Theberge S and Thomas A W 1983 Nucl. Phys. A **393** 252
Thomas A W 1984 Adv. Nucl. Phys. **13** 1
Lu D H, Thomas A W and Williams A G 1998 Phys. Rev. C **57** 2628
[70] Kohyama Y, Oikawa K, Tsushima K and Kubodera K 1987 Phys. Lett. B **186** 255
Tsushima K, Yamaguchi T, Takizawa T M, Kohyama Y and Kubodera K 1988 Phys. Lett. B **205** 128
Tsushima K, Yamaguchi T, Kohyama Y and Kubodera K 1988 Nucl. Phys. A **489** 557
Yamaguchi T, Tsushima K, Kohyama Y and Kubodera K 1989 Nucl. Phys. A **500** 429
[71] Goldberger M L and Treiman S B 1958 Phys. Rev. **110** 1178
[72] Kirchbach K and Wirzba A 1997 Nucl. Phys. A **616** 648
[73] Lu D H, Thomas A W and Tsushima K 2001 arXiv:nucl-th/0112001
Tsushima K, Kim H C and Saito K 2004 Phys. Rev. C **70** 038501
[74] Jones M K*et al.* [Jefferson Lab Hall A Collaboration] 2000 Phys. Rev. Lett. **84** 1398
Gayou O *et al.* [Jefferson Lab Hall A Collaboration] 2002 Phys. Rev. Lett. **88** 092301
[75] Puckett A J R*et al.* 2010 Phys. Rev. Lett. **104** 242301
[76] Arrington J, Melnitchouk W and Tjon J A 2007 Phys. Rev. C **76** 035205
[77] Ostrick M *et al.* 1999 Phys. Rev. Lett. **83** 276
Herberg C *et al.* 1999 Eur. Phys. J. A **5** 131
Glazier D I *et al.* 2005 Eur. Phys. J. A **24** 101
[78] Passchier I *et al.* 1999 Phys. Rev. Lett. **82** 4988
[79] Eden T *et al.* 1994 Phys. Rev. C **50** 1749
[80] Zhu H *et al.* [E93026 Collaboration] 2001 Phys. Rev. Lett. **87** 081801
Warren G *et al.* [Jefferson Lab E93-026 Collaboration] 2004 Phys. Rev. Lett. **92** 042301
[81] Madey R *et al.* [E93-038 Collaboration] 2003 Phys. Rev. Lett. **91** 122002
[82] Riordan S *et al.* 2010 Phys. Rev. Lett. **105** 262302
[83] Schiavilla R and Sick I 2001 Phys. Rev. C **64** 041002
[84] Bosted P E 1995 Phys. Rev. C **51** 409
[85] Kubon G *et al.* 2002 Phys. Lett. B **524** 26
Anklin H *et al.* 1998 Phys. Lett. B **428** 248
Anklin H *et al.* 1994 Phys. Lett. B **336** 313
[86] Lachniet J *et al.* [CLAS Collaboration] 2009 Phys. Rev. Lett. **102** 192001
[87] Zhan X *et al.* 2011 Phys. Lett. B **705** 59
[88] Lin H W and Orginos K 2009 Phys. Rev. D **79** 074507
[89] Eschrich I M G *et al.* [SELEX Collaboration] 2001 Phys. Lett. B **522** 233
[90] Miller G A 2002 Phys. Rev. C **66** 032201
Cloet I C and Miller G A 2012 Phys. Rev. C **86** 015208
[91] Matevosyan H H, Miller G A and Thomas A W 2005 Phys. Rev. C **71** 055204
[92] Lin H W, Cohen S D, Edwards R G, Orginos K and Richards D G 2010 arXiv:1005.0799 [hep-lat]
[93] Gockeler M, Hemmert T R, Horsley R, Pleiter D, Rakow P E L, Schafer A and Schierholz G

[QCDSF Collaboration] 2005 Phys. Rev. D **71** 034508
[94] Alexandrou C, Koutsou G, Negele J W and Tsapalis A 2006 Phys. Rev. D **74** 034508
[95] Alexandrou C *et al.* 2011 Phys. Rev. D **83** 094502
[96] Collins S *et al.* 2011 Phys. Rev. D **84** 074507
[97] Syritsyn S N *et al.* 2010 Phys. Rev. D **81** 034507
[98] Ryu C Y, Hyun C H, Park T S and Hong S W 2009 Phys. Lett. B **674** 122
[99] Plaster B *et al.* [Jefferson Laboratory E93-038 Collaboration] 2006 Phys. Rev. C **73** 025205
[100] Udias J M, Caballero J A, Moya de Guerra E, Amaro J E and Donnelly T W 1999 Phys. Rev. Lett. **83** 5451
[101] Laget J M 1994 Nucl. Phys. A **579** 333
[102] Caballero J A, Donnelly T W, Moya de Guerra E, and Udias J M 1998 Nucl. Phys. A **632** 323
[103] Udias J M and Vignote J R 2000 Phys. Rev. C **62** 034302
[104] Lava P, Ryckebusch J, Van Overmeire B and Strauch S 2005 Phys. Rev. C **71** 014605
[105] Chung P L and Coester F 1991 Phys. Rev. D **44** 229